Ultrasonic Measurement of Suspended Sediment

GEOLOGICAL SURVEY BULLETIN 1141-A

Prepared in cooperation with the Federal Inter-Agency Sedimentation Project

Ultrasonic Measurement of Suspended Sediment

By GORDON H. FLAMMER

CONTRIBUTIONS TO GENERAL GEOLOGY

GEOLOGICAL SURVEY BULLETIN 1141-A

Prepared in cooperation with the Federal Inter-Agency Sedimentation Project

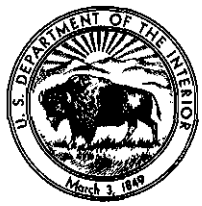

UNITED STATES GOVERNMENT PRINTING OFFICE, WASHINGTON : 1962

UNITED STATES DEPARTMENT OF THE INTERIOR

STEWART L. UDALL, *Secretary*

GEOLOGICAL SURVEY

Thomas B. Nolan, *Director*

For sale by the Superintendent of Documents, U.S. Government Printing Office
Washington 25, D.C.

CONTENTS

ILLUSTRATIONS

TABLE

SYMBOLS

[Pages are those where the symbols are first used]

CONTRIBUTIONS TO GENERAL GEOLOGY

ULTRASONIC MEASUREMENT OF SUSPENDED SEDIMENT

By GORDON H. FLAMMER

ABSTRACT

One of the most serious obstacles to rapid progress in studying the mechanics of sediment movement in streams is the inadequacy of instruments for measuring sediment loads in streams. A new method based on ultrasonic attenuation (decrease in amplitude of the wave from point of origin) by sediment in suspension is presented for determining suspended-sediment size distribution and concentration.

The theoretical study covered three principal items:

1. Existing attenuation relations for an ultrasonic beam passing through a suspension of particles of uniform size were extended to include parameters describing size distribution. The resulting equations gave the attenuation relations for water-sediment mixtures having log-normal size distributions. The log-normal distribution has wide application because it is typical of natural sediments.
2. A method based on the variation of frequency of the sound wave was developed for the unique determination of the log-normal particle-size distribution parameters of an unknown sample.
3. After the particle-size distribution parameters were determined, the sediment concentration was obtained from the attenuation relation for mixtures of sediment sizes.

The experimental study included the following three phases: (a) The attenuation relation for sediment of uniform sieve size was determined for the diffraction-loss and scattering-loss ranges and for the intermediate transition region, for which no satisfactory theoretical equations were available; (b) the theoretical concepts were verified by using the experimental attenuation relations; and (c) some preliminary tests were made of the effects of different types of sediment materials on the relation of attenuation to particle diameter.

Experimental attenuation varied as the 0.33 power of the frequency and inversely as sediment size in the diffraction-loss range and as the 2.4 power of the frequency and the 1.3 power of the size in the transition range.

The sensitivity of measuring the geometric mean size was high, and the sensitivity of measuring standard deviation and concentration would be improved by increasing the range of frequencies to 50 mc (megacycles) or higher.

The ultrasonic method was experimentally verified; however, an extensive equipment-development program is needed to make the instrument operational for laboratory or field use. Also, the effects of sediment properties on ultrasonic attenuation require further study.

INTRODUCTION

A basis phase of the modern scientific revolution has been the advance in measurement techniques, particularly during the past decade or two. The adaptation of electronics to instrumentation has revolutionized many types of measurements, and continued development holds great promise for the future. Such factors as sensitivity of measurement, accuracy, and relative ease of recording are all significant advantages of electronic methods.

One of the most serious limitations in studying the mechanics of sediment movement in a flowing stream has been the lack of adequate measuring instruments. Present methods take only intermittent samples, and the analysis of these samples is laborious and time consuming. As measurement technique improves, the rate of progress in the discovery of the basic principles of sediment-motion mechanics will increase accordingly.

In an attempt to improve the quality and to reduce the cost of records of sediment discharge in streams, the Federal Inter-Agency Sedimentation Project at Minneapolis, Minn. was assigned the tasks of improving sampling methods and equipment and of developing automatic devices for determining sediment concentration and discharge. The immediate objective was to develop an automatic instrument for obtaining, either periodically or continuously, the suspended-sediment concentration at one point in the cross section of a stream. Measuring the attenuations of an ultrasonic beam seemed to be a possible way to determine the concentration of sediment in suspension.

PURPOSE AND SCOPE

The present investigation was made to determine theoretically and experimentally if the attenuations at a few frequencies would define the size distribution uniquely, and if field and laboratory instruments having sufficient accuracy to determine the size distribution could be made. Size distributions are infinitely variable, but a log-normal distribution is typical of natural sediments. Only log-normal distributions are treated in this study so that the size distribution can be defined by two parameters, a geometeric mean particle diameter and the geometric standard deviation. The same methods of investigation could be adapted to other than log-normal distributions whenever some other systematically definable distribution better applies.

After an intensive study of available literature, a method was developed theoretically for defining the two size-distribution parameters by varying the frequency. The sediment concentration could be determined after the size distribution was obtained. The

requirements of an instrument for determining size distribution and concentration of a sediment in suspension were predicted.

Equipment was designed and built for measuring attenuations at frequencies of 2.5, 5.0, 7.5, 12.5, 15, and 25 mc (megacycles). Samples of sediments of known size distribution and concentration were analyzed to find basic attenuation relations for narrow ranges of sediment sizes and for mixtures of sizes, to check theoretical concepts, and to evaluate instrument accuracy. Samples containing sizes smaller than 44 microns could not be tested because of equipment limitations, and sizes larger than 1,000 microns could not be tested without damage to the circulation equipment.

PERSONNEL AND ACKNOWLEDGMENTS

The investigation of the application of ultrasonics to the analysis of sediments in suspension was made in collaboration with the Federal Inter-Agency Sedimentation Project at Minneapolis, Minn. The Inter-Agency Project is guided by a Field Technical Committee under the general supervision of the Subcommittee on Sedimentation of the Federal Inter-Agency Committee on Water Resources. B. C. Colby, project supervisor, and F. S. Witzigman, assistant supervisor, provided supervision and counsel. The report was prepared under the direction of Mr. Colby.

The research work was done at the St. Anthony Falls hydraulic laboratory of the University of Minnesota. The assistance of L. G. Straub, Director of the laboratory and head of civil engineering; J. M. Killen, research engineer; Prof. Edward Silherman; and A. G. Anderson is gratefully acknowledged.

REVIEW OF THEORETICAL CONCEPTS

UNIFORM PARTICLE SIZES

The attenuation of an ultrasonic wave passing through a fluid is greater when suspended particles are present than when they are absent. The basic relation for the increased energy loss that is due to the presence of suspended sediment in a sound field is

$$E = E_0 e^{-2\alpha x} \tag{1}$$

where

E is sound-energy flux at a given point if sediment is suspended in the transmitting fluid
E_0 is sound-energy flux at the same point if no sediment were present
e is base of the Naperian logarithm
α is attenuation coefficient that is due to the sediment alone
x is distance from the point of measurement to the sound source.

644442 O—62——2

The attenuation coefficient α is the logarithm of a power ratio and is measured in nepers per centimeter in the metric system. In the English system

$$E=E_0 10^{-0.1\alpha x} \tag{1a}$$

and α is in decibels per inch. A decibel of attenuation is equivalent to a 20.6-percent decrease in power intensity. A neper equals 8.68 db (decibel), and a neper per centimeter equals 22.05 db per in. In this report all numerical values of α will be in decibels per inch.

The attenuation coefficient α is made up of three loss mechanisms. The first is associated with shear waves (a viscosity phenomenon) set up at the liquid-solid interface because the particle vibrates in response to but lags behind the sound wave. The magnitude of this loss depends on the amount of lag and on the surface area. Extremely small particles tend to move at the same rate as the fluid, and the lag is very small. As size increases, the particles tend to lag more and more behind the movement of the fluid, but at the same time the total surface area of the particles decreases for a constant concentration. These opposing factors result in an attenuation maximum for the "viscous-loss range" (Urick, 1948, p. 284, fig. 1, p. 287). Fluid viscosity and the ratio of particle density to fluid density are likewise important in determining the amount of lag.

The second loss mechanism is the scattering of energy due to a reradiation by the particle of the incident plane wave. The pattern and intensity of the reradiated waves are functions of the ratio of wavelength λ to particle circumference $2\pi r$. For $\lambda>>2\pi r$, the scattering-intensity pattern of a particle is concentrated in the backward directions. As λ approaches $2\pi r$, the scattering distribution becomes more complicated, and the pattern changes rapidly as the frequency changes. For $\lambda<<2\pi r$, half of the scattered wave is concentrated straightforward (the interfering or shadow-forming beam), and the other half is spread out over all other directions. Losses in the "scattering loss range" arise then either from interfering of the scattered wave with the incident wave or from scattering of some of the sound energy from the beam path so that the sound energy fails to reach the point of detection (Morse, 1948, p. 349, 355).

The third loss mechanism arises from losses associated with heat conduction down thermal gradients.[1] It has little significance in this study.

Several theoretical studies have been made to determine the attenuation coefficient α for suspensions of particles of uniform size. The effect of a fixed rigid sphere in a sound field was first studied by Lord

[1] Carhart, R. R., 1950, Theory of viscous and thermal attenuation of sound by small spheres: California Inst. Technology Ph. D. thesis.

Rayleigh (1937). Sewell (1910), Epstein (1941), Urick (1948), and Carhart [2] derived mathematical expressions for the energy loss caused by a single spherical particle in a plane sound field. Sewell assumed the sphere to be rigid and fixed. Both Epstein and Urick considered a rigid sphere that is free to move; and Carhart included also thermal effects, which are important when either the suspended sphere or the suspending medium is highly compressible. In all these studies the wavelength was much greater than the particle circumference ($\lambda >> 2\pi r$). Weinel [3] showed that for solid spheres in water the various expressions for the viscous attenuation are identical. In 1936 Morse (1948, p. 346–357) derived an equation for the scattering of energy by rigid immovable circular cylinders and spheres that were not necessarily small compared with the wavelength. Later, Morse and others (1946) extended the equation to include the effects of compression waves inside the scatterers; the suspended particles were considered to be elastic for both applications. For an elastic sphere, in the region where $\lambda \approx 2\pi r$, Faran (1951) showed that the effect of shear waves in a dense particle must be considered in addition to the effects of compression waves. Anderson (1950) studied the scattering of sound from spherical particles having diameters close to or a few times larger than the wavelength. In his study the specific gravity of the spheres ranged from 0.5 to 2.0, and the sound velocities of the spheres ranged from 0.5 to 2.0 times that of the suspending medium.

Simplifying assumptions are made in order to determine the complex attenuation relations. The first assumption is that the suspended-sediment particles in flowing water are rigid spheres. Anderson (1950, p. 431, fig. 6) compared the scattering cross section for a rigid sphere to that for a sphere of density and sound velocity ratio twice those of the supporting medium. His work indicated that a dense particle whose circumference is less than half the sound wavelength may be considered rigid. Further, he showed that a particle having a specific gravity of 2.0 and a sound velocity twice that of water may be considered rigid for circumference-to-wavelength ratios of 3.0 or greater. Most natural sediments have specific gravities greater than 2 and sound-velocity ratios to water also greater than 2. Therefore, the attenuation relations for rigid particles apply to natural sediment particles except for $0.5 < 2\pi r/\lambda < 3.0$, which will be denoted the transition region. The transition region occurs because the elasticity of the sediment particles has a significant effect in that range. The assumption of a spherical shape is, of course, only an approximation for natural sediments.

The second assumption is that the particles are sufficiently far

[2] Carhart, R. R., 1950, op. cit.

[3] Weinel, C. G., 1953, exploratory study of the measurement of suspended sediment characteristics by sonic means: State Univ. Iowa, M.S. thesis.

apart so that one does not affect the attenuation of another. The computed scattering for a single particle may be multiplied by the number of particles in the sound path to obtain the total scattering. This assumption has been proved valid for $\lambda >> 2\pi r$ by the linear attenuation-concentration relation for concentrations as high as 265,000 ppm by weight (Urick, 1948, p. 286, fig. 5; Busby and Richardson, 1955, p. 193, fig. 2, p. 197). For λ nearly equal to $2\pi r$ the attenuation-concentration relation was still linear for concentrations of 200,000 ppm by weight (Smoltczyk, 1955, p. 37–38, figs. 26–27). For $\lambda << 2\pi r$ no upper limit for this assumption is available, but no evidence of nonlinearity was found for the low concentrations used in this study.

Natural sediments in water are within the rigid classification over much of the range being considered. Expressions for the attenuation coefficient covering the viscous- and scattering-loss ranges have been derived by Sewell, Epstein, Urick, and Carhart, and all are equivalent for rigid particles. Therefore, and because of its relative simplicity, the expression derived by Urick will be used. Carhart's refinement is of no importance here because both the suspending medium and the suspended sediment are incompressible. Urick's expression for the attenuation coefficient is

$$2\alpha = C\left[K(\gamma-1)^2\frac{S}{S^2+(\gamma+\tau)^2}+\frac{K^4r^3}{6}\right]22.05\,\frac{\text{db}}{\text{in.}} \qquad (2)$$

where

C is concentration (1,000 ppm=0.001)
K is equal to $2\pi/\lambda$
γ is equal to ρ_1/ρ_2
S is equal to $[9/(4\beta r)][1+1/(\beta r)]$
τ is equal to $\frac{1}{2}+9/(4\beta r)$
r is particle radius, in centimeters (1 cm=$10^4\,\mu$)
22.05 db per in. is equal to 1 neper per cm.

in which

λ is wavelength of sound in water, in centimeters
ρ_1 and ρ_2 are densities of the particle and fluid, respectively
β is equal to $[\omega/(2\nu)]^{1/2}$
ω is equal to $2\pi f$
ν is kinematic viscosity of the water, in stokes
f is frequency of sound wave.

The first term in equation 2 represents the attenuation due to viscous loss, and the second represents the attenuation due to scattering loss.

Equation 2, which is valid for $\lambda >> 2\pi r$, was used to compute attenuation coefficients for a range of sound frequencies and particle diameters. The results for rigid particles were plotted on figure 1;

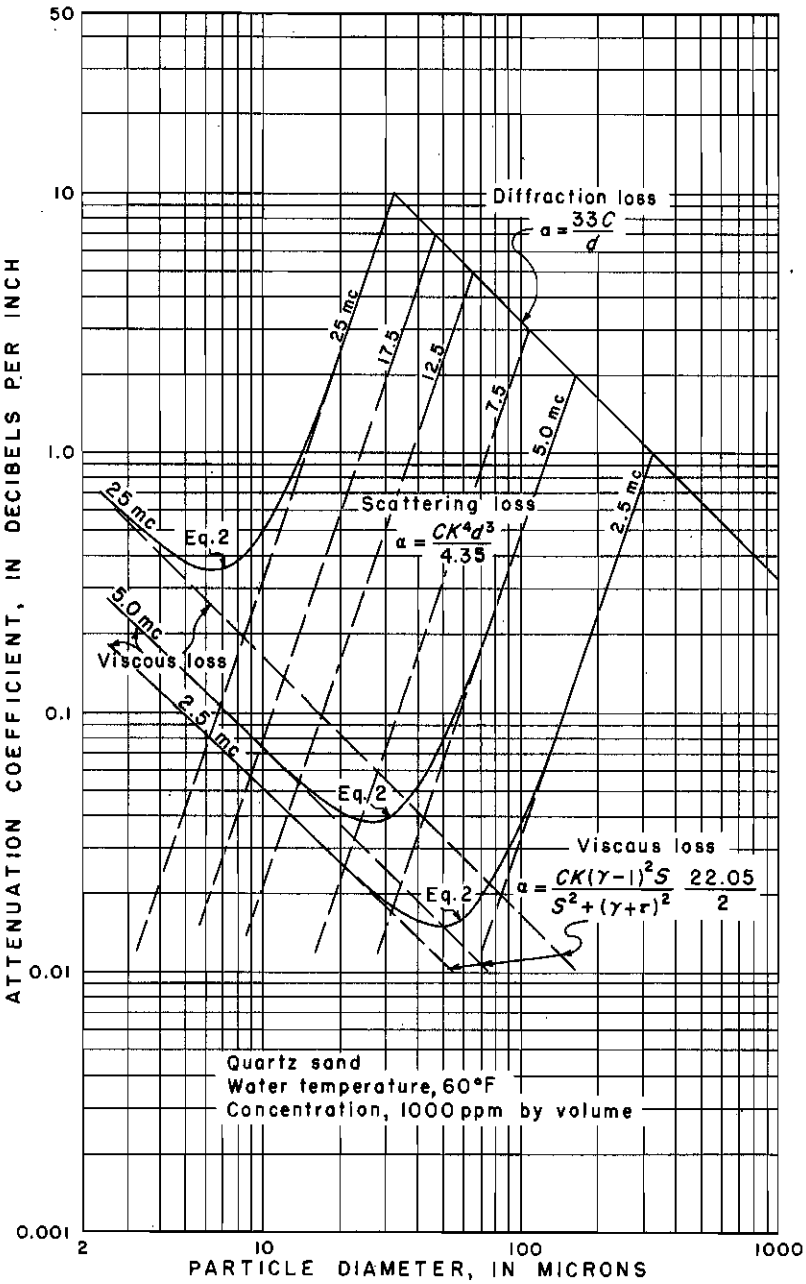

FIGURE 1.—Ultrasonic attenuation by suspensions of rigid particles of uniform size.

therefore, the transition region, which exists for elastic particles, does not appear on this plot. Mathematical expressions for the attenuation coefficient in the transition region involve infinite series and are too complicated to be of practical use in this study.

For $\lambda << 2\pi r$ each particle casts a shadow so that α is proportional to πr^2 (Morse, 1948, p. 355); $\lambda << 2\pi r$ is the diffraction-loss range, and the theoretical expression for the attenuation coefficient is

$$\alpha = n\pi r^2 = \frac{3C}{4\pi r^3}\pi r^2 = \frac{3C}{4r} = \frac{3C}{2d}\frac{\text{nepers}}{\text{cm}} = \frac{33C}{d}\frac{\text{db}}{\text{in.}} \tag{3}$$

where

n is number of particles present per unit volume
d is particle diameter, in centimeters.

Several experimental investigations have been made of the attenuation caused by a sediment suspension in the viscous-loss and scattering-loss ranges. Urick's work (1948) was done mainly in the viscous-loss range at frequencies of from 1 to 15 mc. Stakutis and others (1955) and Busby and Richardson (1955) partly covered both the viscous- and scattering-loss ranges.

Very little experimental investigation has been made in the diffraction-loss range ($\lambda << 2\pi r$). Killen's work [4] was in the diffraction-loss range, and Smoltczyk's results (1955) are for the transition region between the ranges of scattering loss and diffraction loss. Results of the present study cover the diffraction-loss range and the transition region between the diffraction- and scattering-loss ranges.

Comparison of the attenuation relations for light waves and sound waves passing through a suspension of uniform-sized particles may be of interest. The expressions for light as given by Stutz (1930, p. 67–69) are

Scattering loss:

$$\alpha_l = h_1 C K^4 d^3 \text{ for } \lambda >> \pi r \tag{4}$$

Diffraction loss:

$$\alpha_l = \frac{h_2 C}{d} \text{ for } \lambda << 2\pi r \tag{5}$$

Transition region:

$$\alpha_l \text{ is proportional to } K^2 \text{ for } \lambda \approx 2\pi r \tag{6}$$

The first two expressions are identical with the corresponding sound equations for the scattering- and diffraction-loss ranges, except for

[4] Killen, J. M., 1956, The measurement of sediment properties by the scattering of ultrasonic radiation in water: Minnesota Univ. M.S. thesis.

the value of h. Light has no expression corresponding to the ultrasonic viscous loss because light waves do not cause particle vibration as do sound waves. The factor h is a function of the optical or sonic properties of the sediment. Important optical properties, such as color, index of refraction, absorption coefficient, and transparency enter into h, and these properties may vary considerably among natural sediments. Corresponding sonic properties are index of refraction, absorption, and transparency; however, these properties are relatively more uniform among natural sediments.

For the diffraction-loss range of a dielectric, the reflected light is almost independent of wavelength; it is affected only slightly by change in index of refraction with change in wavelength. Theoretical expressions for sonic scattering in the diffraction-loss range also are independent of wavelength.

Of special note is the expression for α in the transition region where $\lambda \approx 2\pi r$ for light. A corresponding expression for the attenuation of sound in the transition region, $\alpha = h_3 K^{2.4} d^x C$, is experimentally derived in this report. (See equation 19, p. A35.)

DISTRIBUTIONS OF PARTICLE SIZES

Generally, sediment suspensions contain particles of many sizes; therefore, development of relations for the sonic attenuation caused by mixtures of sizes is necessary for measuring concentration by the sonic method. An obvious problem is the variety of size-distribution functions necessary to describe all mixtures.

Very little work has been done with mixtures. The use of the sonic-attenuation relations for discrete particle sizes in conjunction with a sedimentation chamber to determine size distribution of mixtures has been suggested by Busby and Richardson (1955, p. 202) and Killen;[5] the use of attenuation relations for light has given varying degrees of success (Traxler and Baum, 1935, p. 466). Grassy (1941) studied the use of the turbidity meter in estimating the suspended load of natural streams.

Gamble and Barnett (1937, p. 311–313, figs. 1–8) varied the wavelength of light through mixtures and found that by plotting percentage of transmission against wavelength, qualitative information on size distribution could be obtained. The shape of the curves indicated very roughly the mean size and the spread of particle sizes. Their results were not quantitative.

Smoltczyk (1955) studied simple mixtures. He first found the sonic attenuations caused by several uniform sizes—actually he used fractions of narrow size ranges obtained by sieving—then took

[5] Killen, J. M., 1956, op. cit.

two of these fractions, mixed them in a variety of proportions, and found the attenuation caused by the mixtures. The relation obtained was

$$E=E_0e^{-2(\alpha_1+\alpha_2)x} \tag{7}$$

where

α_1 is attenuation coefficient due to the presence of size fraction 1 in the suspension

α_2 is attenuation coefficient due to the presence of size fraction 2.

This relation further verifies the basic assumption that the particles are far enough apart so there is no interaction or interference between them. Smoltczyk also studied the relationship of the attenuation coefficient to frequency for a given size fraction (250 to 300 μ). The transducer frequencies he used were 1, 2, 3, and 4 mc.

THEORETICAL DEVELOPMENT

In order to use the ultrasonic method for measuring concentration and size distribution, parameters that define size distribution must be included in the equations. The size parameters will be based on an assumed distribution, such as the normal distribution. The usual normal-probability equation applies only to distributions that are symmetrical about a vertical axis; therefore, it does not apply to most natural sediments, the distributions of which are asymmetrical or skewed. However, for the majority of natural sediments the frequency curves are normal if the logarithm of the size is substituted for the size. The truth of this statement is verified by the fact that their distributions when plotted on log-probability paper yield straight lines, except at the extremes. The deviation at the extremes is unimportant because the areas under the curves extending from the points of deviation to infinity are negligible compared to the total area under the curves between the largest and smallest particles measured (DallaValle, 1948, p. 53–54). Not only most natural sediments (Hatch and Choate, 1929, p. 379; Einstein, 1944, figs. 9 and 29; Blench, 1952, p. 147; Chow, 1954, p. 2; Colby and Hembree, 1955, figs. 13 and 32) but also the products of many manufacturing and chemical processes, such as those from crushing and grinding and chemical precipitation (Austin, 1939, figs. 3–7; Hatch and Choate, 1929, p. 380–383), are log normal. Thus, this distribution has wide application. The important parameters describing the straight-line plot on log-probability paper are d_g, the geometric mean, which is the 50-percent size, and σ_g, the geometric standard deviation, which is the ratio of the 84.13-percent size to the 50-percent size or of the 50-percent size to the 15.87-percent size.

The equation of the normal-frequency size distribution is

$$\phi(d)=\frac{\Sigma n}{\sigma\sqrt{2\pi}}\,e^{-\frac{(d-\bar{d})^2}{2\sigma^2}} \tag{8}$$

where

d is particle diameter

$\bar{d}$ is arithmetic mean particle diameter

σ is standard deviation and is equal to $\sqrt{\frac{\Sigma[n(d-\bar{d})^2]}{\Sigma n}}$

For an asymmetric distribution, the logarithms of the sizes are substituted for the sizes:

$$\phi(\ln d)=\frac{\Sigma n}{\ln \sigma_g\sqrt{2\pi}}\,e^{-\frac{(\ln d-\ln d_g)^2}{2\ln^2\sigma_g}} \tag{9}$$

$$\ln \sigma_g=\sqrt{\frac{\Sigma[n(\ln d-\ln d_g)^2]}{\Sigma n}}$$

Because $\phi(\ln d)$ fits most natural sediments, it was chosen as the distribution function for this study.

The basic relation necessary to include the size-distribution parameters in the attenuation equation is

$$\alpha_T=\int_0^\infty \alpha'(d)\phi(d)dd \tag{10}$$

where

α_T is attenuation coefficient for a mixture of discrete particle sizes

$\alpha'(d)$ is attenuation coefficient for size d per unit concentration by volume

$\phi(d)$ is size-frequency distribution;

or for a log-normal distribution

$$\alpha_T=\int_{-\infty}^{\infty} \alpha'(d)\phi(\ln d)d(\ln d) \tag{11}$$

Equations 10 and 11 follow directly from the assumption that the particles are sufficiently far apart so that one does not affect the attenuation of another.

The attenuation coefficient has three loss ranges; therefore, three different integrals have to be evaluated. (Urick's relation will be used.)

1. Viscous-loss range:

$$\alpha_T=\phi(\lambda,\ \rho_1,\ \rho_2,\ d_g,\ \sigma_g,\ \nu,\ C) \tag{12}$$

$$\alpha'(d)=\frac{K}{2}(\gamma-1)^2\frac{S}{S^2+(\gamma+\tau)^2}22.05\frac{db}{\text{in.}} \tag{2}$$

which is the first part of equation 2. By substituting,

$$\alpha_T=\int_{-\infty}^{\infty}\frac{a\frac{K}{2}(\gamma-1)^2\frac{9}{2\beta d}\left[1+\frac{2}{\beta d}\right]C\,e^{-\frac{(\ln d-\ln d_g)^2}{2\ln^2\sigma_g}}}{\frac{81}{4\beta^2d^2}\left[1+\frac{2}{\beta d}\right]^2+\left[\gamma+\frac{1}{2}+\frac{9}{2\beta d}\right]^2}d(\ln d)$$

which becomes after some manipulation:

$$\alpha_T=\int_{-\infty}^{\infty}\frac{a_6[d^3+2\beta d^2]C\,e^{-\frac{(\ln d-\ln d_g)^2}{2\ln^2\sigma_g}}}{a_1d^4+a_2d^3+a_3d^2+a_4d+a_5}d(\ln d) \tag{13}$$

where the a's are constants for a given sediment in water under standard conditions and for a given frequency.

Equation 13 seems to require numerical integration by means of a computer. As this study will not extend into the viscous-loss range, no attempt was made to evaluate the equation.

2. Scattering-loss range:

$$\alpha_T=\phi(\lambda,\ d_g,\ \sigma_g,\ C) \tag{14}$$

$$\alpha'(d)=\frac{K^4d^3}{4.35}=\frac{358.5d^3}{\lambda^4}\frac{db}{\text{in.}} \tag{2}$$

$$\alpha_T=\int_{-\infty}^{\infty}\frac{358.5d^3C\,e^{-\frac{(\ln d-\ln d_g)^2}{2\ln^2\sigma_g}}}{\lambda^4\ln\sigma_g\sqrt{2\pi}}d(\ln d)$$

making the substitution $u=\ln d$

$$\alpha_T=a_7e^{(4.5\ln^2\sigma_g+3\ln d_g)}\int_{-\infty}^{\infty}e^{-\frac{1}{2\ln^2\sigma_g}[u-(\ln d_g+3\ln^2\sigma_g)]^2}du$$

making another substitution, $w=u-(\ln d_g+3\ln^2\sigma_g)$

$$\alpha_T=a_7e^{(4.5\ln^2\sigma_g+3\ln d_g)}\int_{-\infty}^{\infty}e^{-\frac{w^2}{2\ln^2\sigma_g}}dw$$

with the final result:

$$\alpha_T = \frac{358.5 d_g^3 C}{\lambda^4} e^{4.5 \ln^2 \sigma_g} \tag{15}$$

3. Diffraction-loss range:

$$\alpha_T = \phi(d_g, \sigma_g, C) \tag{16}$$

$$\alpha'(d) = \frac{33}{d} \frac{db}{\text{inch}} \tag{3}$$

$$\alpha_T = \int_{-\infty}^{\infty} \frac{33C\, e^{-\frac{(\ln d - \ln d_g)^2}{2 \ln^2 \sigma_g}}}{d \ln \sigma_g \sqrt{2\pi}}\, d(\ln d)$$

which becomes by substituting $u = \ln d$

$$\alpha_T = a_g e^{(\frac{1}{2} \ln^2 \sigma_g - \ln d_g)} \int_{-\infty}^{\infty} C\, e^{-\frac{1}{2 \ln^2 \sigma_g} [u - (\ln d_g - \ln^2 \sigma_g)]^2}\, du$$

By substituting $v = u - (\ln d_g - \ln^2 \sigma_g)$

$$\alpha_T = a_g e^{(\frac{1}{2} \ln^2 \sigma_g - \ln d_g)} C \int_{-\infty}^{\infty} e^{-\frac{v^2}{2 \ln^2 \sigma_g}}\, dv$$

which integrates to

$$\alpha_T = \frac{33C}{d_g} e^{\frac{1}{2} \ln^2 \sigma_g} \tag{17}$$

Equations 15 and 17 for the scattering- and diffraction-loss ranges, respectively, include size-distribution parameters so they apply to mixtures of particles that have log-normal distributions. Either of these equations will give the attenuation for rigid particles if the sizes for any given distribution are entirely within either the scattering-loss or the diffraction-loss range. For suspensions having sizes in both ranges, equation 11 must be numerically integrated. The procedure used for integration is as follows:

1. Log-normal size distributions for a wide range of d_g and σ_g are plotted on log-probability paper. From the plots the concentrations and mean sizes of the arbitrarily chosen size increments are read. The concentration increments are based on a total concentration of 1,000 ppm.
2. The attenuation coefficient for the mean size of each increment is read from figure 1 for each frequency.
3. Then α_T was computed as $\Sigma \alpha'(d) C(d)$ for each size distribution and frequency. $C(d)$ is the concentration of size d material.

The resulting curves are shown on figure 2. The solid lines show

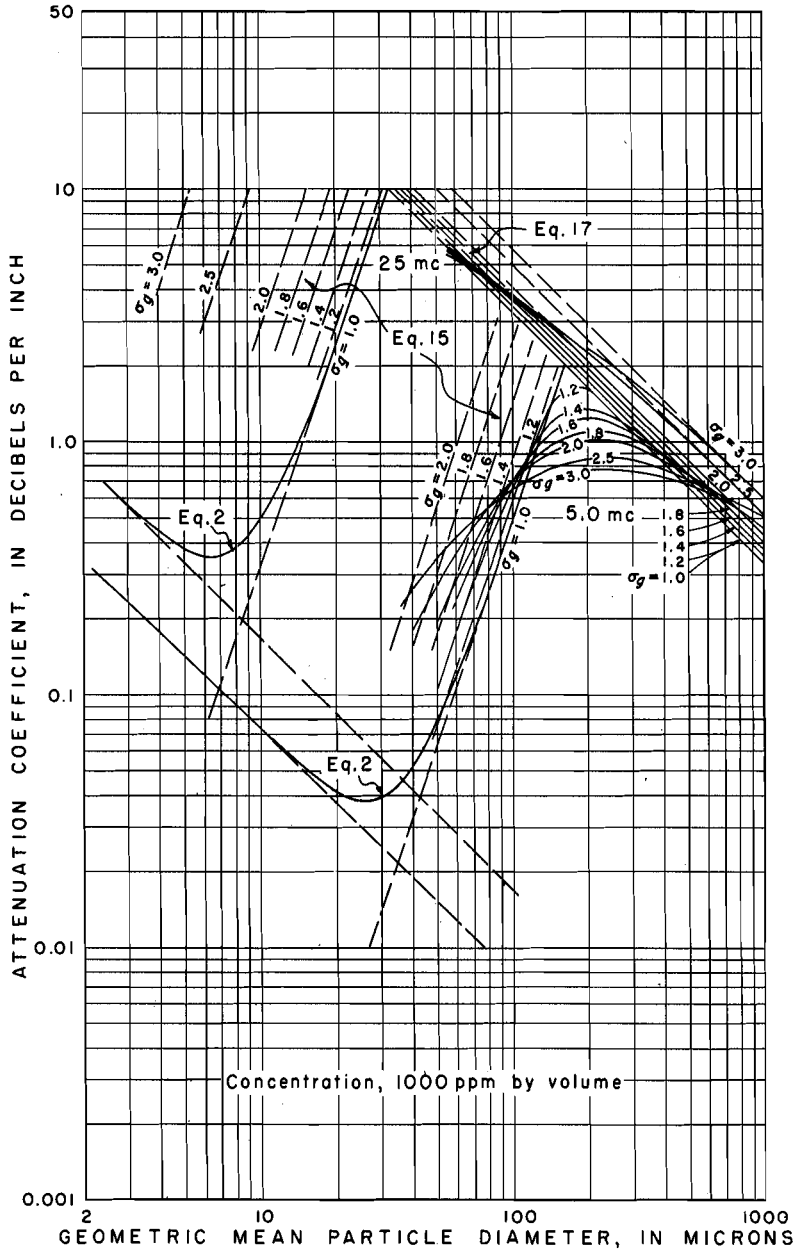

FIGURE 2.—Ultrasonic attenuation for mixtures of rigid particles having a log-normal size distribution and falling within the scattering- and diffraction-loss ranges.

the results of the numerical integration, and these lines approach asymptotically the dashed lines, which are plots of equations 15 and 17.

For the initial phases of this study no relations were available for the transition region (for elastic particles) from the scattering-loss to diffraction-loss ranges ($0.5<2\pi r/\lambda<3.0$), so the particles were assumed to be rigid, and the scattering-loss curves of figure 1 were arbitrarily extended to intersect the diffraction-loss curves. Extension of the curves was necessary to obtain the attenuation values for step 2 above. Thus, because the transition region was ignored, the original evaluation of equation 11 was only approximate; however, plots of this equation showed the attenuation-versus-frequency curve to be unique for a given size distribution. On the basis of these results, experimental apparatus was constructed so the attenuation relations for the transition region could be obtained.

After construction of the experimental apparatus (p. A29), the attenuation coefficients for size fractions from a mixture of Missouri River sand and blasting sand (M.S. mixture) were measured; the results were plotted on figure 3, which shows the experimental curves corresponding to the theoretical curves of figure 1. The procedure for numerical integration of equation 11 was then repeated by using the data in figure 3 instead of figure 1. Many numerical evaluations were made because several variables were involved. The values covered by the variables in the integration were as follows:

d_g=75, 100, 125, 150, 175, 200, 250, 300, 400, and 500 microns
σ_g=1.0, 1.4, 1.6, 1.8, 2.0, 2.5, and 3.0
f=2.5, 5.0, 7.5, 12.5, 15, and 25 mc
C=1,000 ppm

The concentration was not varied because the attenuation-concentration relation is linear. The sonic velocity, which is very nearly the same in the suspensions as in water (Stakutis and others, 1955, p. 541), was taken as 1,475 meters per second; therefore, for the frequencies used the corresponding wavelengths were 590, 295, 197, 118, 98, and 59 microns. Figures 4, 5, and 6 indicate the results of the numerical analysis. From these figures the attenuation of a sonic plane wave at a given frequency is read for any desired size distribution. This attenuation is for a concentration of 1,000 ppm; however, because the attenuation-concentration relation is linear, the attenuation at any concentration is obtained by multiplying the attenuation read from the figures by the ratio of the desired concentration to the 1,000-ppm concentration.

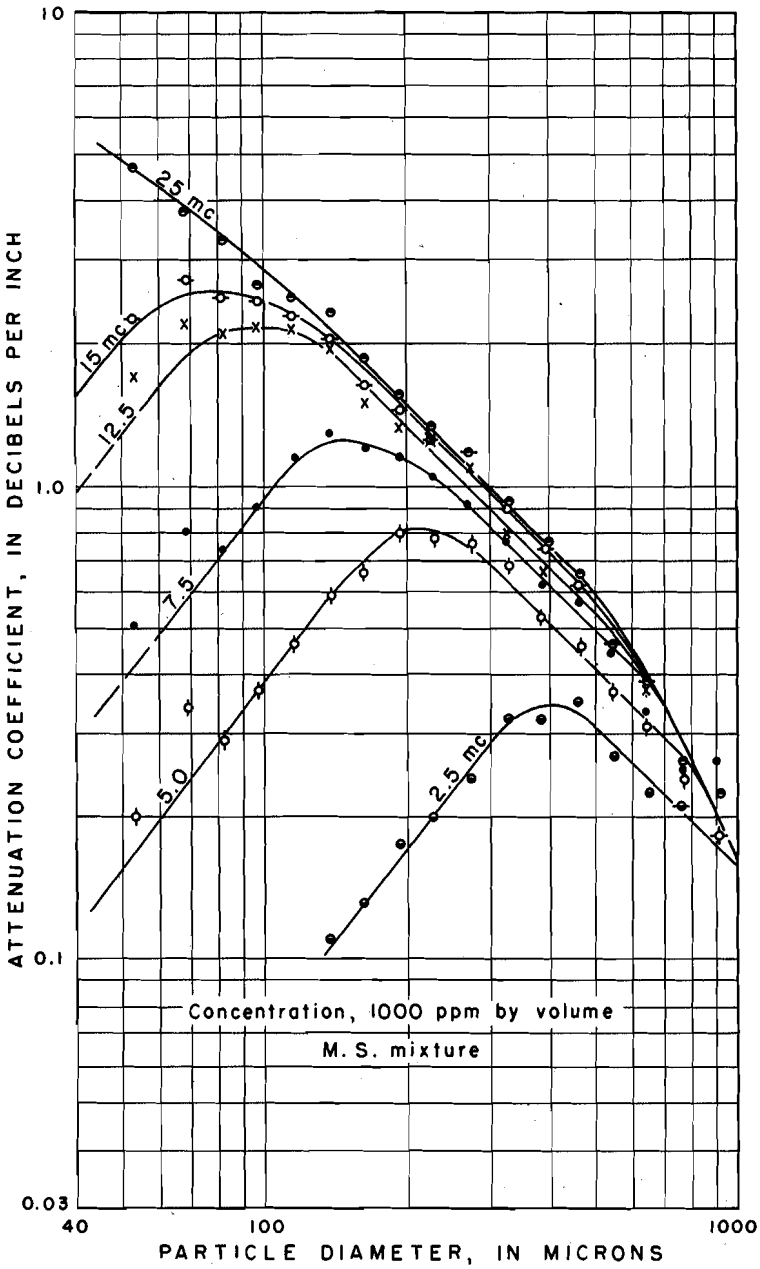

FIGURE 3.—Experimental results for ultrasonic attenuation by size fractions made up from Missouri River sand and blasting sand.

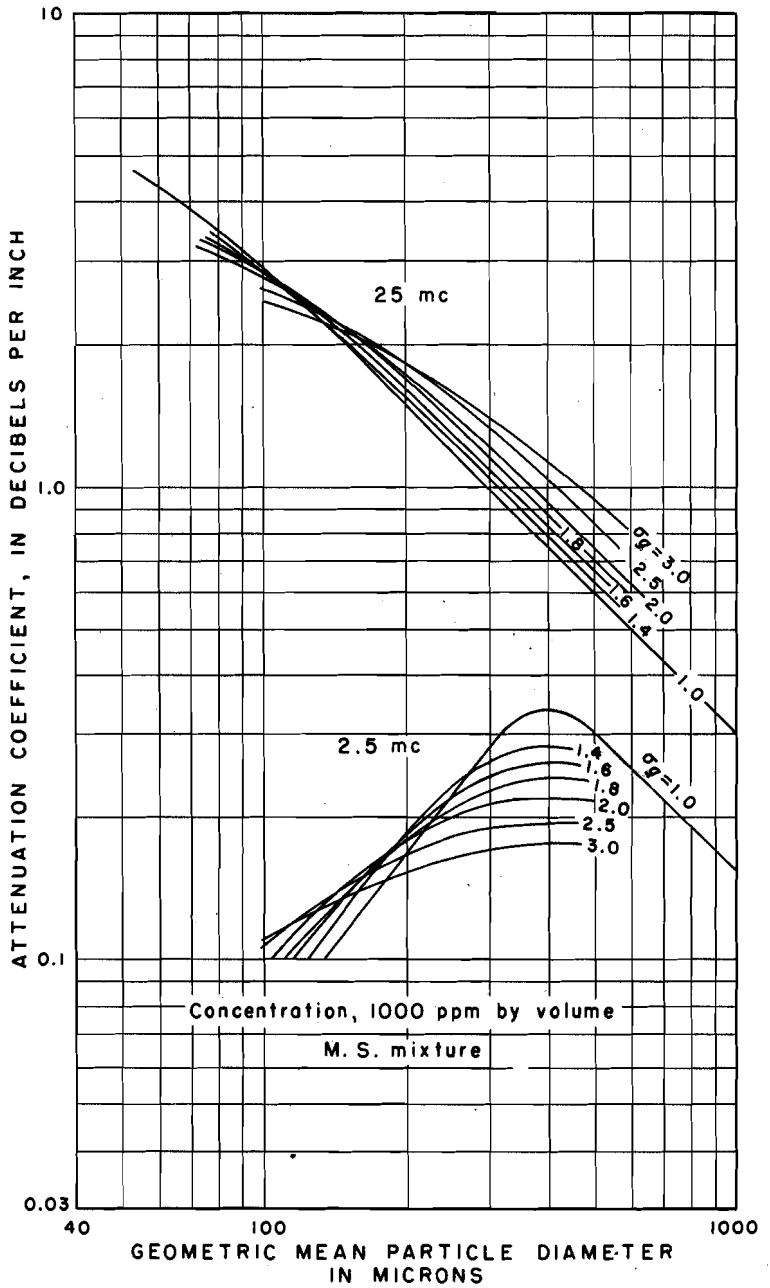

FIGURE 4.—Ultrasonic attenuation at 2.5 and 25 mc for mixtures having a log-normal size distribution.

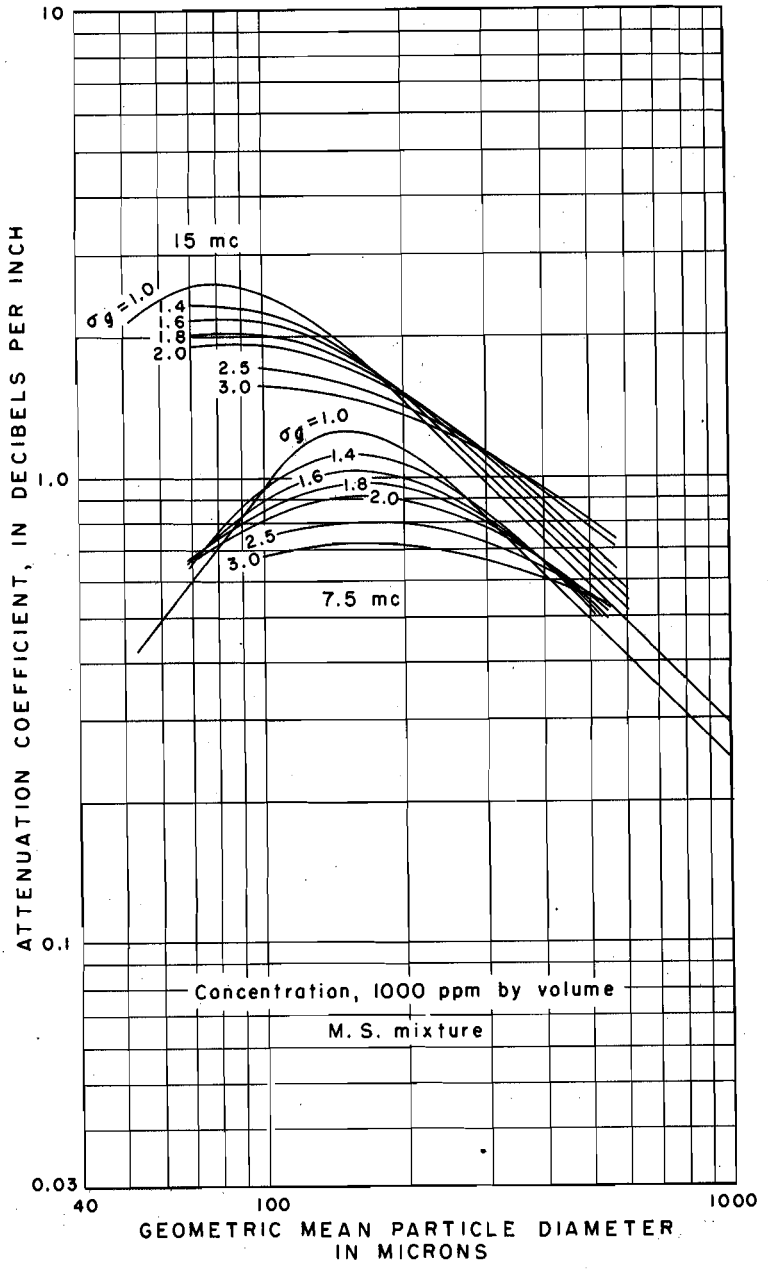

FIGURE 5.—Ultrasonic attenuation at 7.5 and 15 mc for mixtures having a log-normal size distribution.

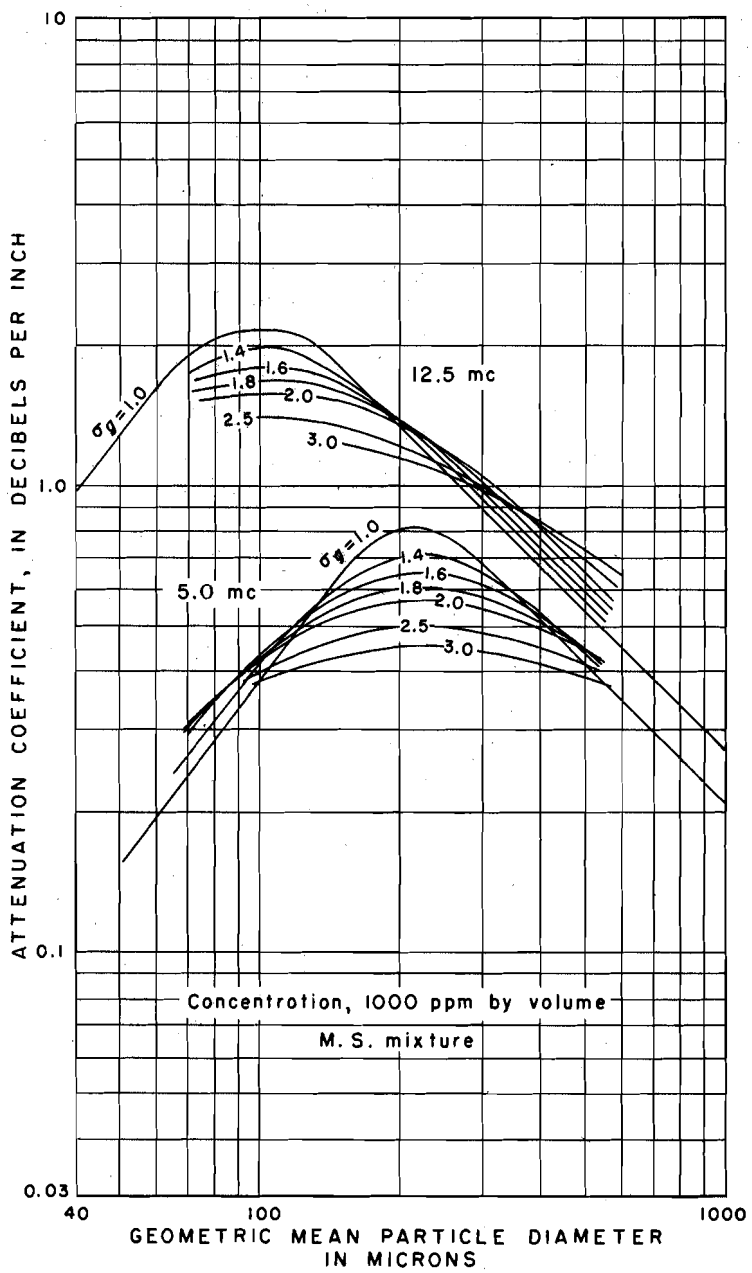

FIGURE 6.—Ultrasonic attenuation at 5.0 and 12.5 mc for mixtures having a log-normal size distribution.

644442 O—62——4

Because of its linear relation to attenuation, concentration may be eliminated as a variable by using a ratio of the attenuation for a given frequency (α_f) to the attenuation for a frequency of 25 mc (α_{25}). The reference chosen for the ratios is the attenuation for the highest frequency used (25 mc) because the sensitivity of attenuation measurement increases as the frequency increases. Figures 7 through 14 were obtained by plotting α_f/α_{25} against transducer frequency and by using d_g and σ_g as parameters. These figures show that the curve for any given combination of d_g and σ_g is unique.

When the size distribution of a given sediment suspension has been determined, the concentration may be obtained from figures 4, 5, or 6.

The laboratory measurement of an unknown sediment sample would proceed as follows:

1. The attenuation of the altrasonic beam passing through a suspension containing sediment of unknown size distribution and concentration is read and recorded for each of several specified frequencies.
2. The recorded attenuations are then divided by the attenuation for 25 mc and plotted against frequency on log paper of the same scale as figures 7 to 12. The plotted curve is placed, in turn, over figures 7 to 12 to find a matching curve, from which d_g and σ_g are read.
3. The values of d_g and σ_g are then used to enter figures 4 to 6, from which the attenuation per 1,000-ppm concentration at any desired frequency is read; the highest frequency will give the greatest measurement sensitivity. The unknown concentration of the sample is obtained by dividing this attenuation into the attenuation recorded at the desired frequency and multiplying by 1,000.

Thus, the size distribution and concentration for any log-normal sediment sample falling in the scattering-loss and diffraction-loss ranges may be determined. The extension of the relations into the viscous-loss range would follow the same procedure as outlined for the other two ranges.

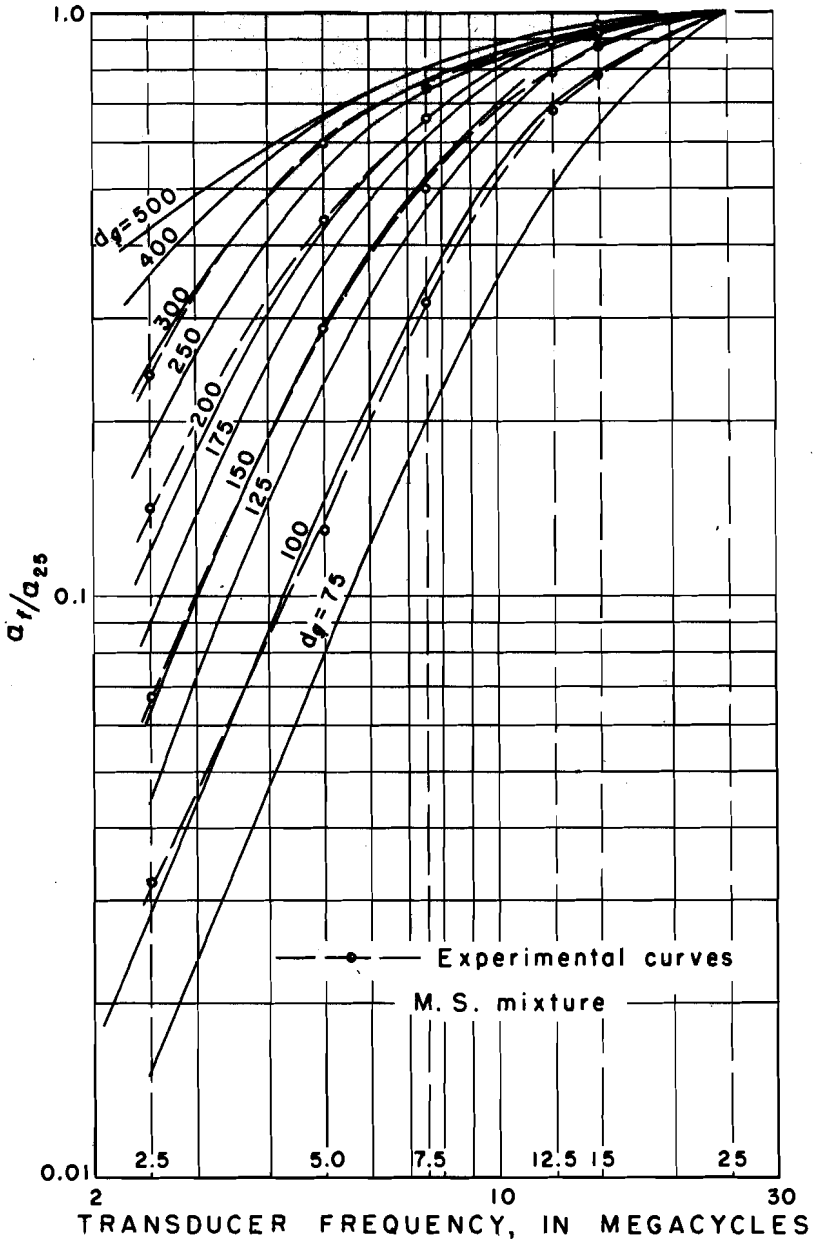

FIGURE 7.—Curves for the determination of the size-distribution parameters d_g and σ_g, for σ_g equal to 1.4.

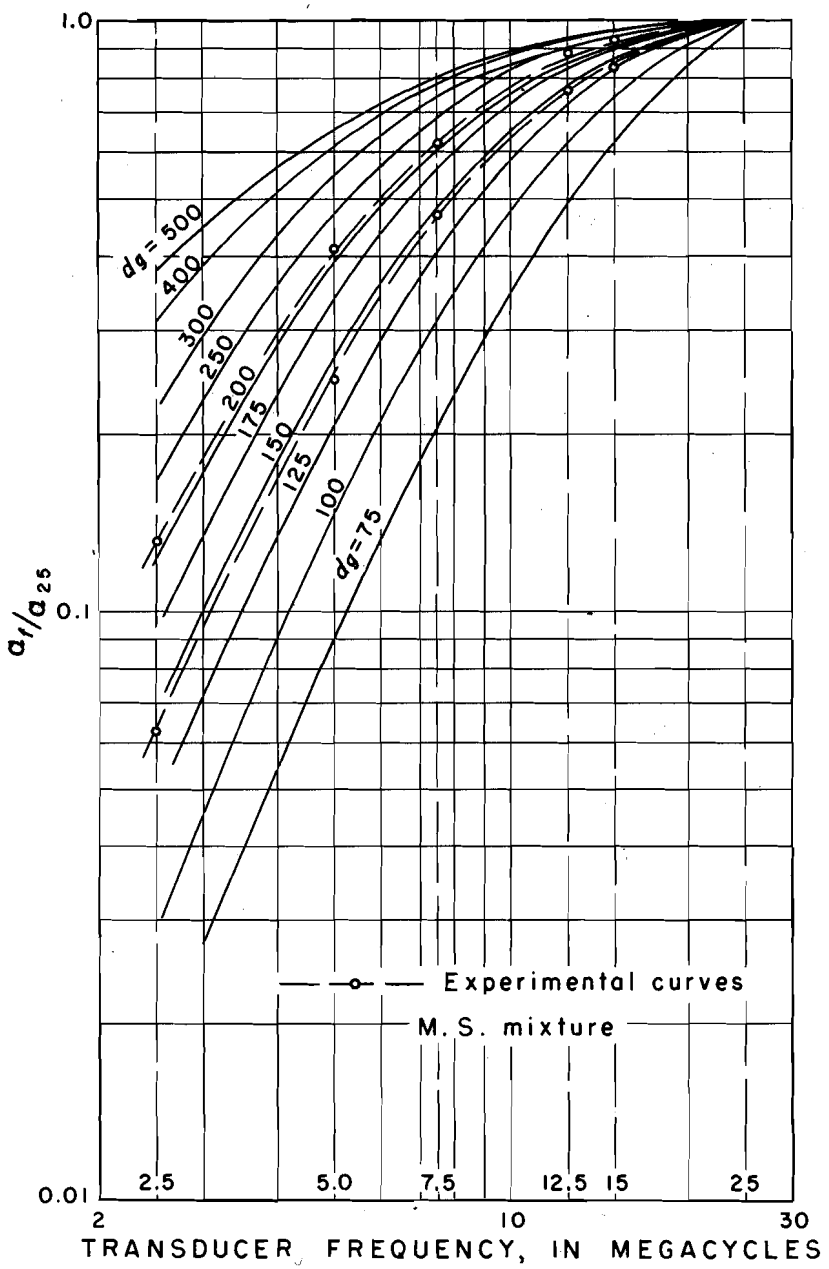

FIGURE 8.—Curves for the determination of the size-distribution parameters d_g and σ_g, for σ_g equal to 1.6.

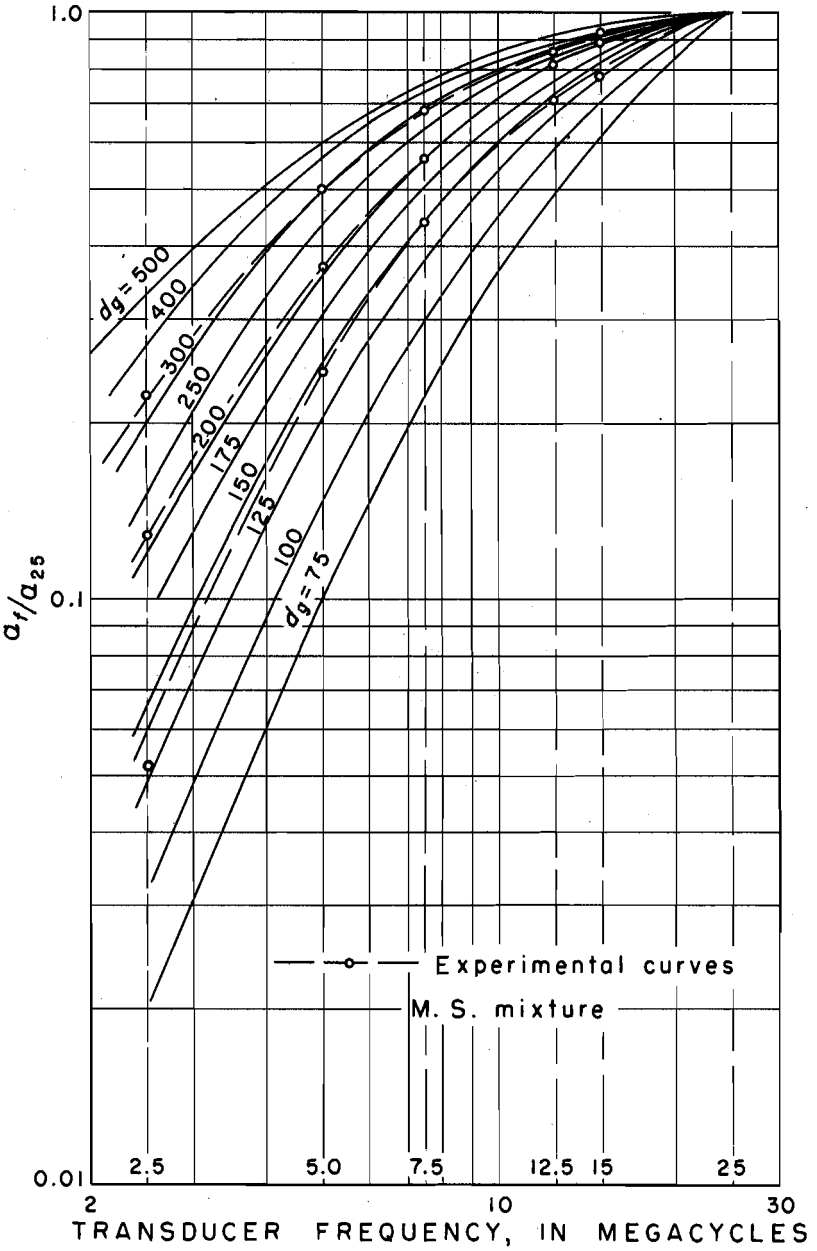

FIGURE 9.—Curves for the determination of the size-distribution parameters d_g and σ_g, for σ_g equal to 1.8.

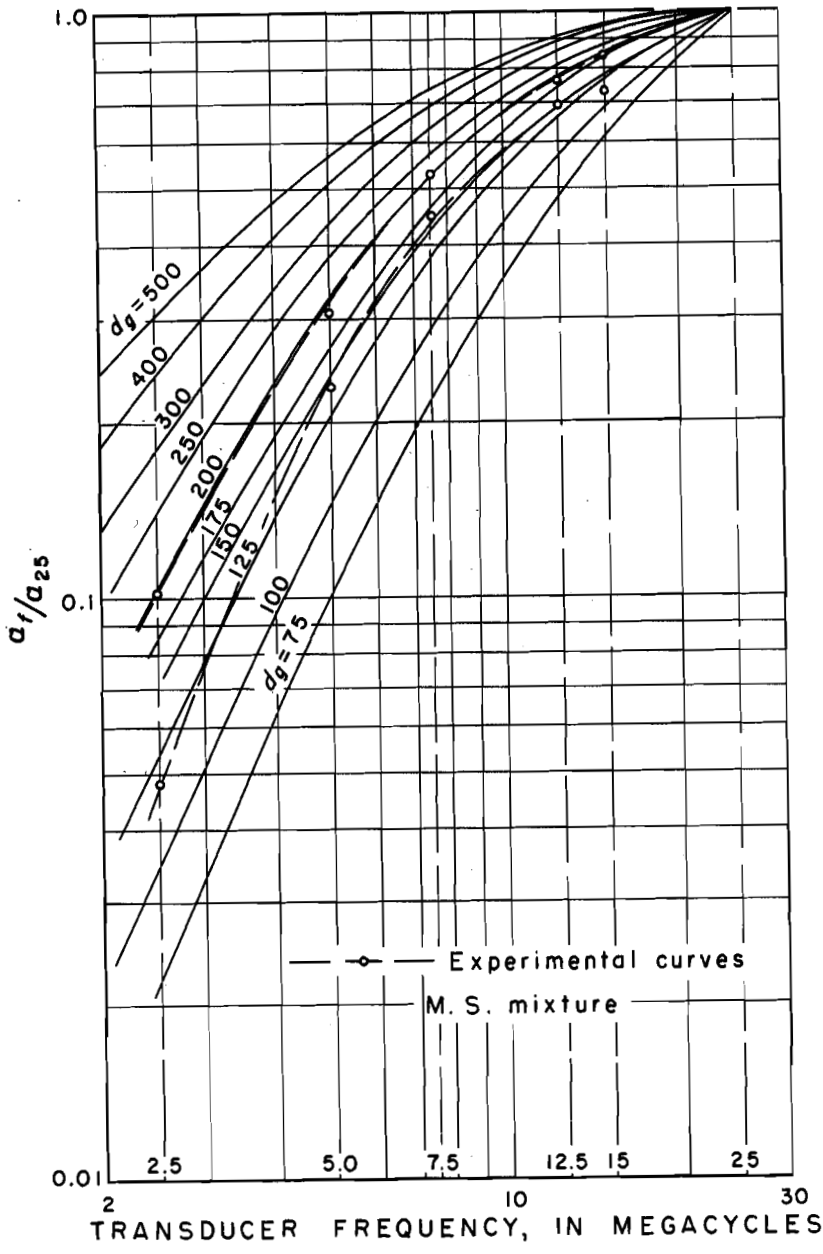

FIGURE 10.—Curves for the determination of the size-distribution parameters d_g and σ_g, for σ_g equal to 2.0.

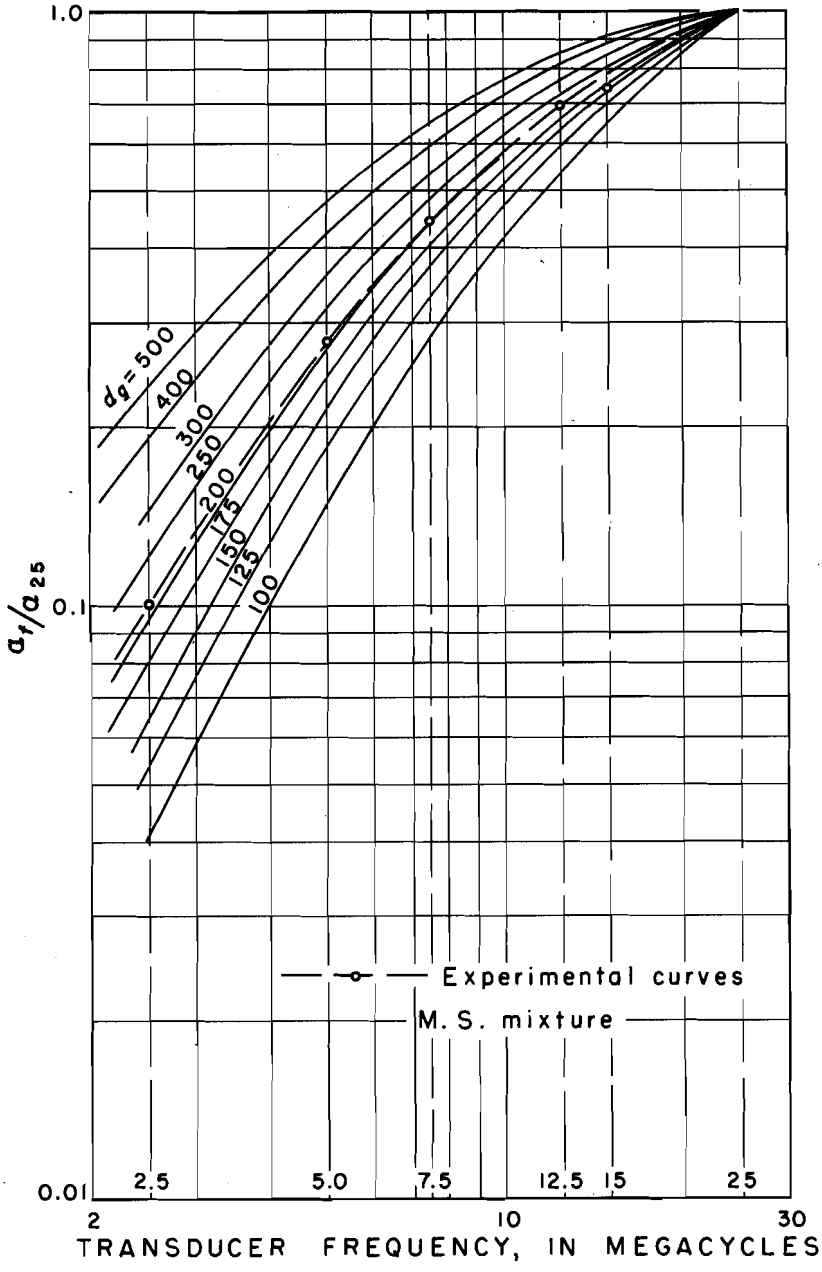

FIGURE 11.—Curves for the determination of the size-distribution parameters d_g and σ_g, for σ_g equal to 2.5.

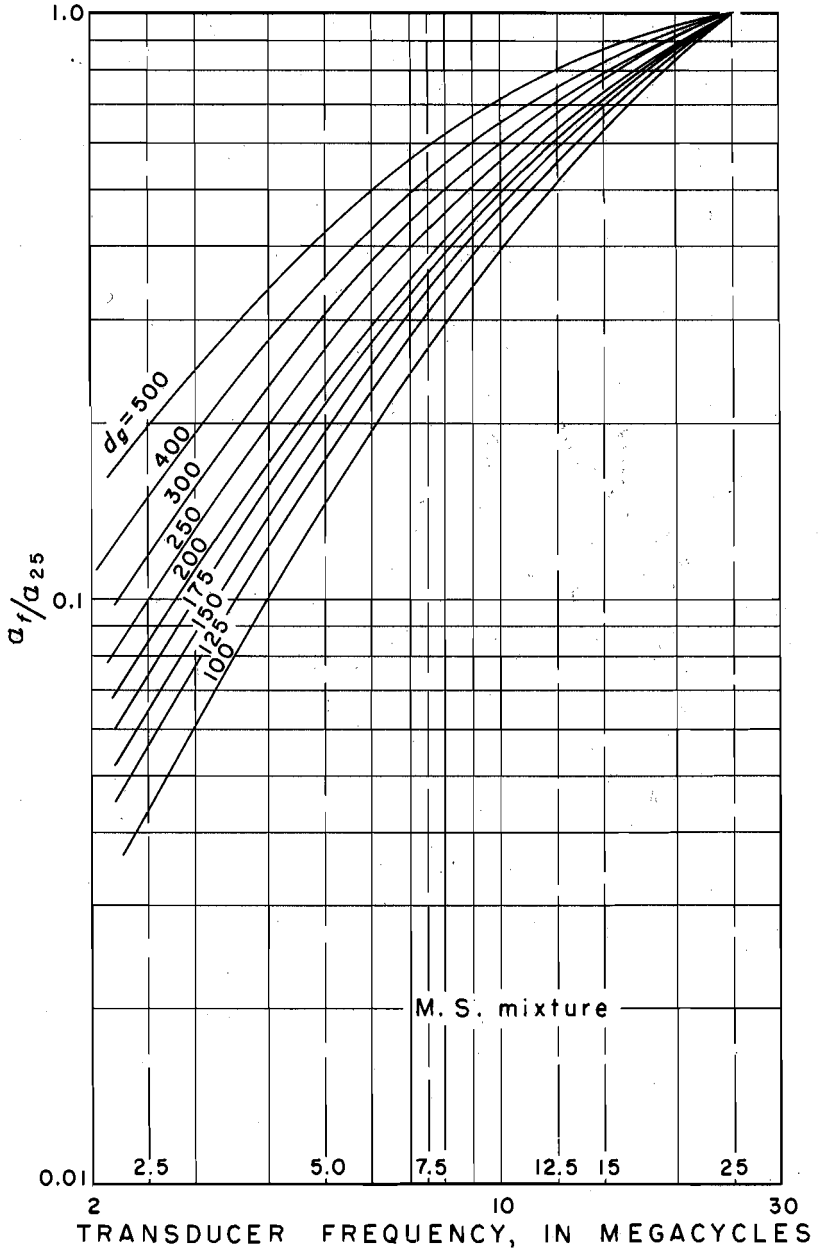

FIGURE 12.—Curves for the determination of the size-distribution parameters d_g and σ_g, for σ_g equal to 3.0.

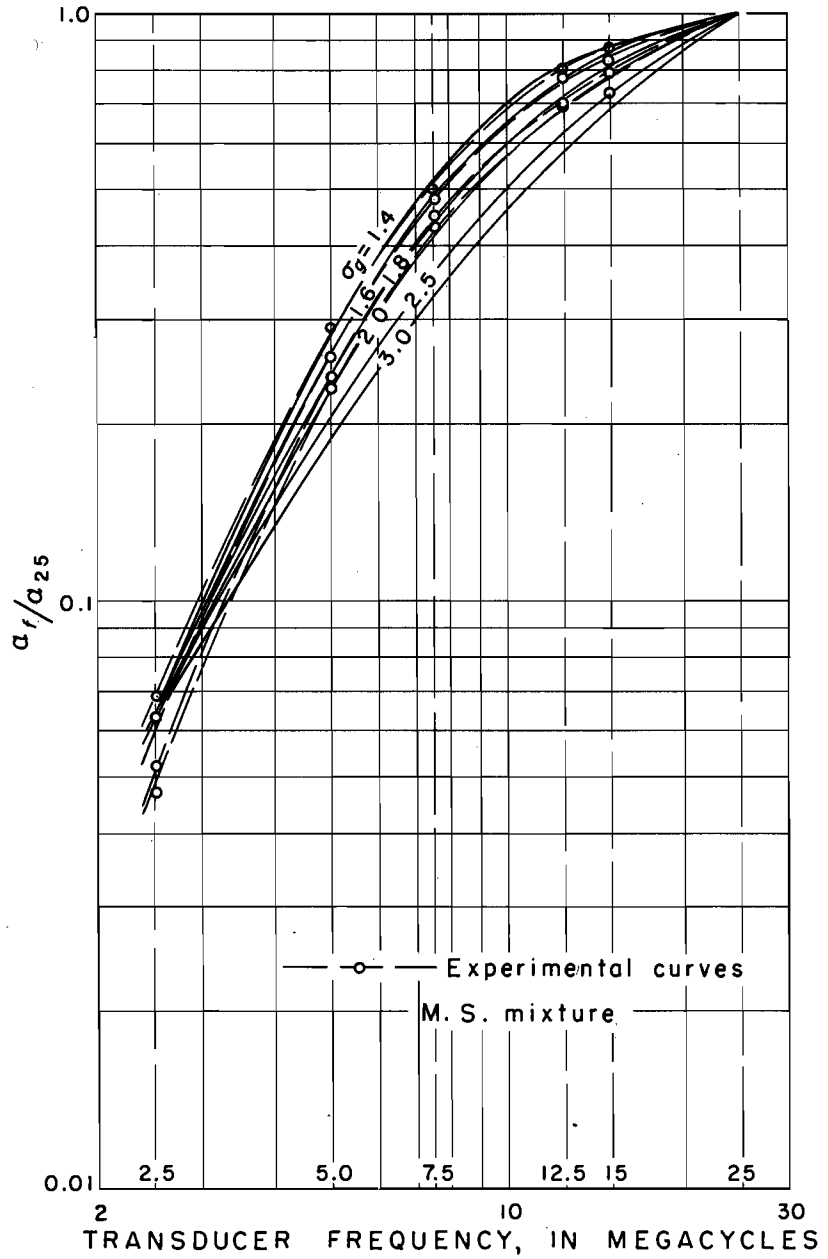

FIGURE 13.—Curves showing the sensitivity of measurement of the geometric standard deviation, for d_f equal to 150 microns.

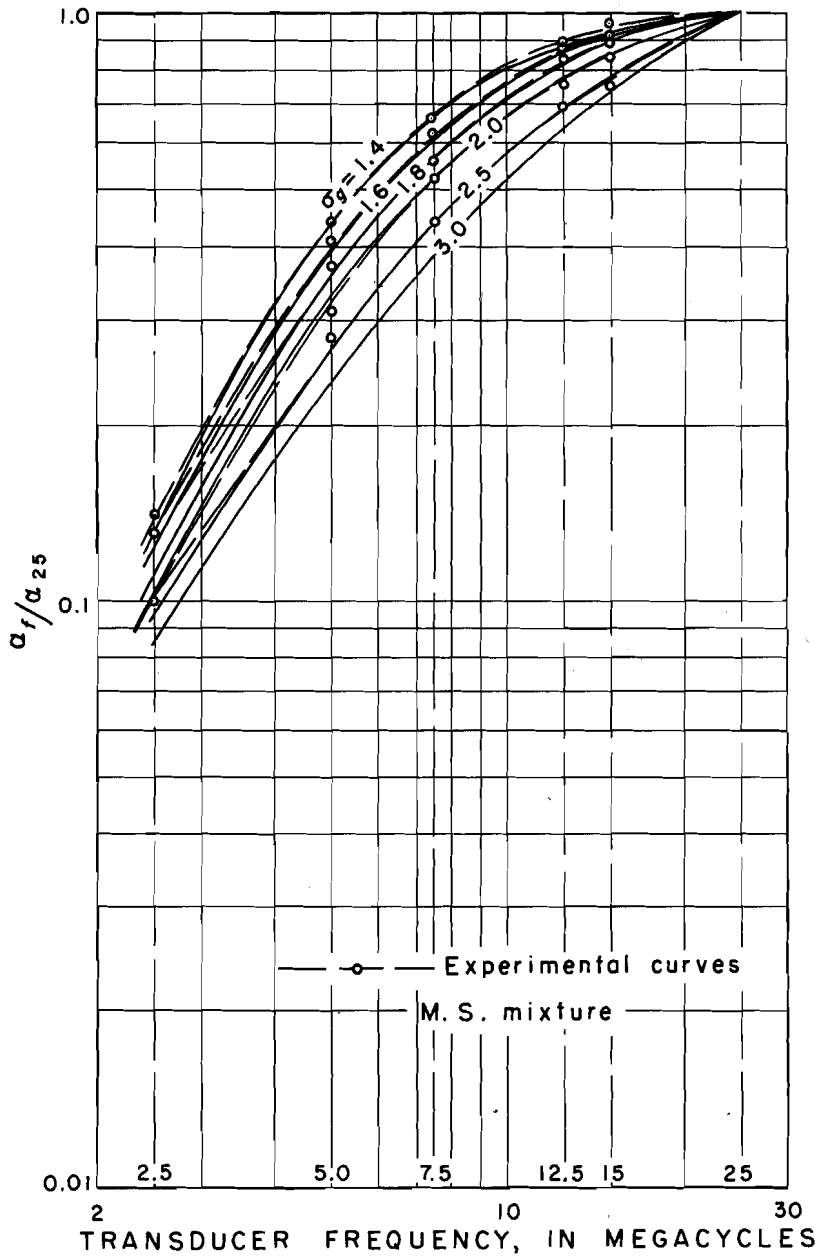

FIGURE 14.—Curves showing the sensitivity of measurement of the geometric standard deviation, d_g equal to 200 microns.

EXPERIMENTAL APPARATUS AND PROCEDURES

A block diagram of the experimental apparatus is shown on figure 15. The equipment is based on the same principles as depth sounders or underwater suhmarine-detection devices; however, the attenuation is measured instead of range, and considerably higher frequencies are used.

The pulse generator actuates the transmitter for 6 microseconds at a repetition rate of 200 times per second, and it simultaneously triggers the oscilloscope sweep. The transmitter drives an x-cut quartz crystal, which transforms the electric wave into a pressure wave. This ultrasonic pressure wave travels as a plane wave across the sediment chamber to the reflector and back to the crystal. The returning echo is transformed by the crystal into an electric wave, which then passes through an attenuator into the receiver and appears on the oscilloscope. (See figs. 16–18.)

Plug-in transmitter units generate the frequencies, and each plug-in unit is designed to operate at a specific frequency. Because only odd harmonics of the quartz crystals are usable, the first, third, and fifth harmonics of the 2.5- and 5.0-mc crystals were used. Higher harmonics were very much desired, but funds and power output were limited. Not only does the power output from the crystal decrease with the higher order harmonics, but the attenuation due to the water in the sediment chamber increases as the square of the frequency; therefore, as the frequency increases, the power output must be increased. The upper limit for power output is determined by the occurrence of cavitation in the water. The highest of the six frequencies used in this study was 25 mc.

The crystal and reflector faces must be parallel to each other. Both lateral and longitudinal adjustments of these components were made by means of thumbscrews on spring-loaded bolts through backing plates (figs. 15, 16). The longitudinal adjustment is principally to place the components flush with the chamber walls for minimum flow disturbance.

The sediment chamber is rectangular (3 by 3 in.) and has fillets in each corner to reduce corner effects on flow. The shape was most convenient to construct, especially for the refleetor and crystal ports. Clear-plastic walls allow observation of the flow.

The concentration in the vicinity of the ultrasonic beam path should be as uniform and steady as possible; therefore, a recirculating system is used. The mixture is pumped from the bottom of the chamber through a plastic hose and discharges into the top of the chamber through 10 holes in the hose wall; the end of the hose is plugged (fig. 15). The jets from these holes cause extreme turbulence,

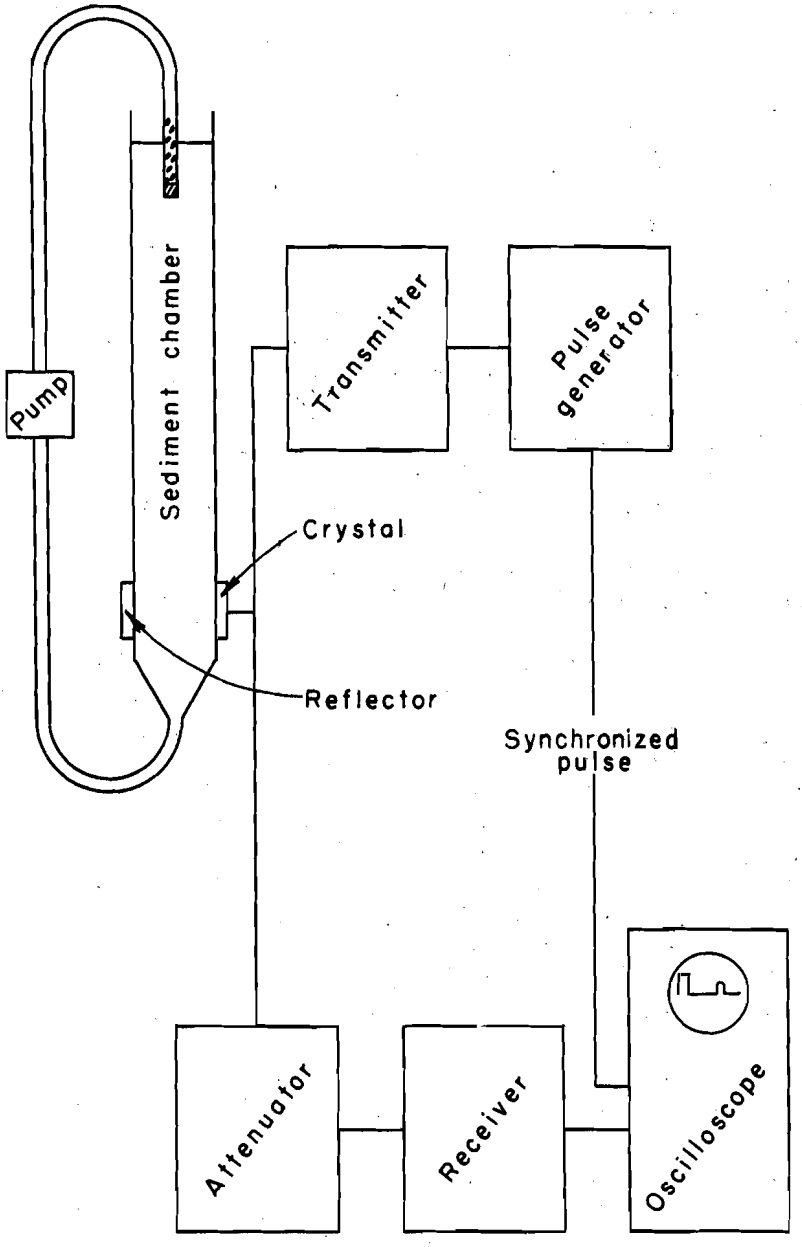

FIGURE 15.—Block diagram of ultrasonic apparatus.

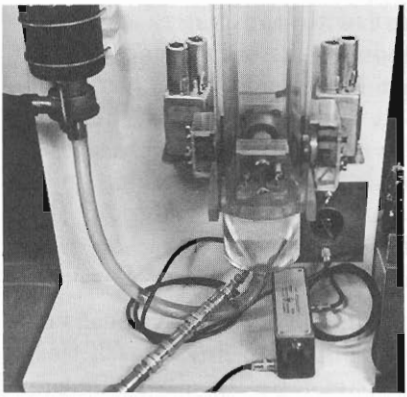

FIGURE 16.—Plug-in transmitter units, crystal and reflector holders, and attenuator.

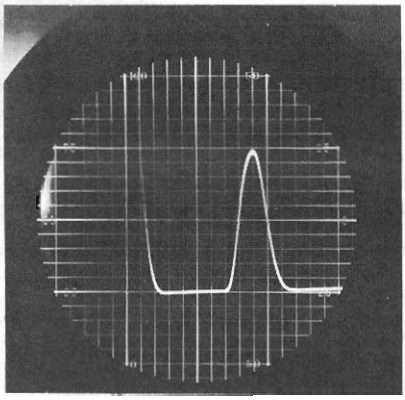

FIGURE 17.—Transmitter pulse edge and echo on oscilloscope.

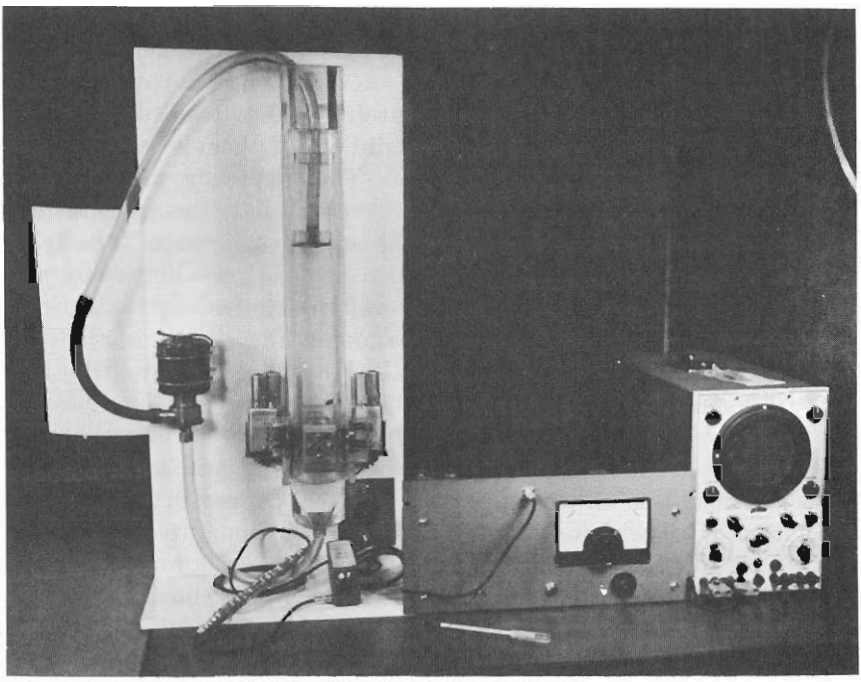

FIGURE 18.—General layout: recirculating sediment chamber, transmitter, receiver, attenuator, and oscilloscope.

PHOTOGRAPHS SHOWING EXPERIMENTAL APPARATUS

which thoroughly mixes the sediment with the water. A double screen just below the inlet section reduces the turbulence. Steady flow is attained rapidly (within about 10 seconds). A clear-plastic transition at the bottom converges to fit the suction hose of the pump.

The attenuator is a commercially available unit and measures up to 32 db, in 1-db steps. It has a flat-frequency response up to 500 mc. The receiver is of standard superheterodyne design. The oscilloscope is a commercial unit and has good stability characteristics.

The operating procedure for a typical test proceeds as follows:

1. The sediment chamber is filled with distilled water by means of a siphon. Care must be taken during filling to entrain as little air as possible because entrained air attenuates the ultrasonic wave more strongly than does the sediment. After the chamber is filled to a prescribed level, the pump is freed of air by operating it in short bursts and allowing sufficient time intervals between for all air bubbles to rise to the surface. The pump discharge hose is placed deep enough below the surface so no air is entrained by vortexes and yet shallow enough so the concentration is uniform up to the surface. Actually, because of the care taken, little trouble was encountered with entrained air.
2. Two transmitter units are plugged in; one of them is transmitting while the other is warming up. The frequency that is being transmitted is tuned in on the receiver dial; the transmitters may require retuning. After the apparatus is tuned, the echo trace on the oscilloscope is set to an arbitrary height by adjusting the attenuator and the volume control on the oscilloscope. The amount of attenuation in the circuit is read; as much attenuation is placed in the circuit as is allowed by the transmitter power output and the chosen trace height.
3. After the trace is set the pump is shut off, and the sediment sample is introduced at the top of the chamber. Again care must be taken not to entrain air; the sample is poured in slowly, and time is allowed for trapped air bubbles to come to the surface. The finer samples are more inclined to trap air bubbles, however, no difficulty was encountered when the above procedure was followed.
4. After all air bubbles drawn into the water by the sediment sample return to the surface, the pump is turned on. When the concentration becomes uniform, the echo becomes relatively steady; but the echo has decreased because of the additional energy loss caused by the presence of the sediment. The trace is adjusted back to its original height by changing the attenuator to decrease the attenuation in the electric circuit. The amount of the decrease is the additional attenuation of the ultrasonic beam

caused by the suspended sediment. Any effect of nonlinearities in the receiver or oscilloscope or of dissolved solids in the fluid is eliminated by confining the measurement to the effect of sediment only.

5. Because drift of some of the transmitter frequencies is sometimes a problem, each run is checked by shutting off the pump after the test and allowing the sediment to settle. If no drift has occurred, the trace will return to its original height with the initial attenuation. If any drift is found, the sample is rerun. Of course, short-time drift might not be detected.
6. When a test is completed, the recirculating system is thoroughly washed out, in preparation for the next run.

The first step in the experimental program was to obtain the relation of attenuation coefficient to particle size for the six frequencies. Size fractions having as narrow a spread of sizes as possible were required. An investigation of methods for obtaining size fractions indicated that sieving would probably be the most suitable. The range of particle sizes from 44 to 1,000 microns was broken into 17 fractions, whose σ_g was less than 1.2. Because figure 2 shows that the attenuation coefficient for size distributions having a σ_g equal to 1.2 is very nearly the same as for σ_g equal to 1.0, these fractions were considered to be narrow enough for testing.

The samples were all sieved twice. For the first sieving the sand was placed on the top sieve of the nest and run in the sieve shaker for 15 minutes. The fractions were collected in separate jars. Then for the second sieving about 5 grams from each jar was placed on the sieve above the one on which it was originally retained and again run in the shaker for 15 minutes. The inherent inaccuracies of sieving undoubtedly account for at least part of the experimental scatter.

Size fractions were obtained in this way for Minnesota silica sand, blasting sand, and a mixture of Missouri River sand and blasting sand. The mixture was necessary to obtain sufficient amounts of each size fraction.

Some sand fractions that had been prepared by other experimenters were available. Because tests on these fractions were run prior to the design and construction of the present variable-frequency apparatus, they were run at only one frequency, 25 mc. The sands are Cheyenne River sand, Taylors Falls sand, Republican River sand, Powder River sand, and a specially mixed sand.

Other materials available in size fractions were glass beads and abrasive grits of aluminum oxide and of silicon carbide. The glass beads were sieved according to the above method, but the size range of the abrasive grits was considered to be narrow enough in range to forego the added labor of sieving. The σ_g of the grit was less than 1.2

except for the very fine grits, which were far below the sieving range.

All these materials have been used in this study, although only the M.S. mixture was thoroughly tested. The others will aid in research extending beyond this study.

DISCUSSION OF RESULTS

Figure 3 shows the results of the M.S. mixture size-fraction tests for the six frequencies. A comparison of this figure with figure 1, which shows the theoretical curves for the scattering- and diffraction-loss ranges, reveals some interesting differences.

The theoretical relation for the diffraction-loss range is independent of frequency, whereas figure 3 indicates that attenuation is dependent on frequency. Similar plots, not included in this study, for Minnesota silica sand, aluminum oxide abrasive grits, and glass beads also indicated frequency dependence. The theoretical relation for the diffraction-loss range is

$$\alpha=\frac{33C}{d}\frac{db}{\text{in.}} \tag{3}$$

or for C=1,000 ppm,

$$\alpha=\frac{0.033}{d}$$

The empirical relation for the M.S. mixture for this range is

$$\alpha=\frac{0.122f^{1/3}C}{d}=\frac{6.4C}{d\lambda^{1/3}} \tag{18}$$

or for C=1,000 ppm,

$$\alpha=\frac{0.000122f^{1/3}}{d}$$

$$\alpha=\frac{0.0064}{d\lambda^{1/3}}$$

where f is the transducer frequency in cycles per second.

The experimental diffraction-loss curves of figure 3 begin to deviate from a straight-line relation at about 500 microns for 25 mc and at increasingly larger sizes for lower frequencies. The curves seem to approach independence of frequency near the 1,000-micron size, though additional data for sizes greater than 1,000 microns are needed to determine the relation conclusively. Accurate measurement is rather difficult to achieve for these large sizes owing to the unsteadiness of the echo.

Anderson's results (1950) indicate that the transition region between the scattering- and diffraction-loss ranges extends from $0.5<2\pi r/\lambda<$

3.0 for each frequency. For each of the six frequencies used, the range of sizes in the transition region is as follows:

Frequency (megacycles)	*Particle-diameter range (microns)*
2.5	94–560
5.0	46–282
7.5	31–188
12.5	19–112
15.0	16– 94
25.0	9– 56

For all the frequencies except 2.5 mc the smallest size tested was still in the transition region. Theoretically, the lower limit of the transition region would approach the scattering-loss curves; however, the lower limit for 2.5 mc does not appear to do so. A possible explanation may be that the transition regions from diffraction loss to scattering loss and from scattering loss to viscous loss overlap for 2.5 mc. Unfortunately, no size fractions were available in the M.S. mixture smaller than 44 to 62 microns. Furthermore, the equipment limitations were most evident at the small sizes, the testing of which involved long periods with attendant drift.

The empirical expression for the straight-line part of the transition-region curves of figure 3 for the M.S. mixture is

$$\alpha = 0.36K^{2.4}d^{1.3}C \tag{19}$$

or for $C = 1{,}000$ ppm,

$$\alpha = 0.00036K^{2.4}d^{1.3}$$

In the expression for the attenuation of light in the transition region, where $\lambda \approx 2\pi r$, α_l is proportional to K^2 (equation 6, p. A8). This equation further shows the similarity between light and sound attenuations.

Artificial mixtures were made up from the size fractions of the M.S. mixture to test the theoretical propositions. The following size distributions were mixed and tested:

Geometric mean size (microns)	*Geometric standard deviation*
100	1.4
150	1.4, 1.6, 1.8, 2.0
200	1.4, 1.6, 1.8, 2.0, 2.5
300	1.4, 1.8
500	1.4

Table 1 shows α_r for the experimental and integrated values for these distributions for a concentration of 1,000 ppm. Only 5 of 95 experimental readings differed by more than 10 percent from the integrated values; the 2.5-mc readings are excepted here because they are so small in magnitude that their accuracy is poor.

TABLE 1.—*Experimental and integrated values of the attenuation coefficient for a concentration of 1,000 ppm* [1]

Geometric mean size (micron)	Geometric standard deviation	Method	Attenuation coefficients (decibels per inch) at a transducer frequency of—					
			2.5 mc	5.0 mc	7.5 mc	12.5 mc	15 mc	25 mc
100	1.4	Integrated	0.078	0.41	0.95	2.00	2.26	2.82
			.028	.15	.34	.71	.81	1.00
		Experimental	.090	.37	.92	1.98	2.23	2.85
			.032	.13	.32	.69	.78	1.00
150	1.4	Integrated	.13	.61	1.11	1.71	1.84	2.07
			.063	.29	.54	.83	.89	1.00
		Experimental	.14	.57	1.02	1.63	1.81	[2] 2.15
			.065	.27	.47	.70	.84	1.00
		do	.15	.59	1.06	1.71	1.86	[2, 3] 2.33
			.065	.25	.46	.74	.80	1.00
		do	.14	.60	1.02	1.65	1.79	[2] 2.24
			.063	.27	.46	.74	.80	1.00
		do	.16	.66	1.04	1.70	1.83	2.11
			.076	.31	.49	.81	.87	1.00
		do	.136	.60	1.02	1.61	1.71	2.04
			.067	.29	.50	.79	.84	1.00
		Mean-Experimental	.14	.60	1.03	1.66	1.80	2.07
			.068	.29	.50	.80	.87	1.00
150	1.6	Integrated	.14	.58	1.04	1.67	1.83	2.13
			.066	.27	.49	.78	.80	1.00
		Experimental	.13	.54	1.00	1.69	1.81	[2] 2.22
			.059	.24	.48	.76	.82	1.00
		do	.13	.58	.99	1.66	1.80	[2] 2.29
			.057	.25	.43	.72	.79	1.00
		do	.17	.56	1.04	1.72	1.81	2.04
			.083	.27	.51	.84	.89	1.00
		Mean-Experimental	0.13	0.56	1.03	1.67	1.81	2.18
			.063	.26	.47	.77	.83	1.00
150	1.8	Integrated	.14	.55	.97	1.61	1.78	2.19
			.064	.25	.44	.74	.81	1.00
		Experimental	.11	.51	.91	1.47	1.64	2.10
			.052	.24	.43	.70	.78	1.00
150	2.0	Integrated	.14	.52	.92	1.54	1.72	2.18
			.064	.24	.42	.71	.79	1.00
		Experimental	.10	.48	.95	1.45	[3] 1.54	2.11
			.047	.23	.45	.69	.73	1.00
200	1.4	Integrated	.19	.69	1.06	1.39	1.48	1.59
			.12	.43	.67	.87	.93	1.00
		Experimental	.21	.68	1.01	1.37	1.48	1.54
			.14	.44	.66	.89	.96	1.00
200	1.6	Integrated	.19	.64	1.00	1.39	1.49	1.64
			.12	.39	.61	.88	.91	1.00
		Experimental	.20	[3] .55	.97	1.38	1.44	1.57
			.13	.41	.62	.88	.92	1.00
200	1.8	Integrated	.18	.60	.95	1.37	1.49	1.67
			.11	.36	.57	.82	.89	1.00
		Experimental	.21	.60	.90	1.32	1.43	1.60
			.13	.37	.56	.83	.89	1.00
200	2.0	Integrated	.18	.56	.89	1.35	1.48	1.72
			.10	.33	.52	.78	.86	1.00
		Experimental	.18	.54	.90	1.29	1.44	1.72
			.10	.31	.52	.75	.84	1.00
260	2.5	Integrated	.17	.50	.80	1.22	1.42	1.82
			.093	.27	.44	.67	.78	1.00
		Experimental	.18	.50	.79	1.24	1.35	1.80
			.10	.28	.44	.69	.75	1.00
300	1.4	Integrated	.26	.66	.84	.94	1.03	1.07
			.25	.61	.78	.88	.96	1.00
		Experimental	.25	.62	[3] .75	.94	.96	1.04
			.24	.60	.72	.90	.92	1.00
300	1.8	Integrated	.23	.58	.81	1.01	1.10	1.17
			.20	.50	.69	.86	.94	1.00
		Experimental	.24	.56	.75	.93	1.02	1.11
			.22	.50	.68	.84	.92	1.00
500	1.4	Integrated	.28	.43	.53	.57	.62	.64
			.43	.67	.82	.89	.96	1.00
		Experimental	.31	.44	.52	.57	.57	[3] .57
			.54	.77	.91	1.00	1.00	1.00

[1] Two values are recorded: the first is for α_f; the second is for α_f/α_{25}.
[2] Error due to transmitter-frequency drift at higher concentrations.
[3] Indicates that experimental values differ from integrated values by more than 10 percent.

Table 1 also shows the α_f/α_{25} for the experimental and integrated values, representative curves of which are shown on figures 7 to 14. Data for the series in which d_g is equal to 150 microns were inconsistent at first. Comparison with the integrated values showed that the experimental readings at 25 mc were in error. Investigation indicated that at the higher concentrations the frequency of the transmitter shifted slightly so the receiver was no longer exactly in tune and the attenuation reading was too large.

For the tests of mixtures, concentrations were varied with frequency. At the higher frequencies the maximum concentration was limited by the power output available, and at the lower frequencies the minimum concentration was limited by the increased accuracy desired. The limitations resulted in the use of a low concentration for the highest frequency and a high concentration for the lowest frequency. Table 1 shows the results of the attenuation readings at various concentrations adjusted to 1,000 ppm for each frequency. The adjustment is not strictly valid because all the factors entering into the measurement error, such as the drift, are not proportional to concentration. However, in spite of ignoring these factors, most of the experimental results agree within 10 percent of the integrated values; therefore, figures 4 to 6 may be considered sufficiently accurate for concentration determination.

Figures 7 to 12 indicate that for a given geometric standard deviation, the sensitivity of measuring the different geometric mean sizes with the method is high. Also, the agreement between the experimental and integrated data is reasonably good.

Figures 13 and 14 indicate that for 150 and 200 microns, the sensitivity of measuring the different geometric standard deviations with the method is not as high as that for the geometric mean sizes. The curves are so close together that the experimental equipment inaccuracies are more serious, especially if the highest frequency used is at all unstable, because all other attenuations are divided by this frequency.

The sensitivity of measurement may be increased by using a frequency higher than 25 mc. Figures 19 and 20 are theoretical plots for the same geometric mean sizes and geometric standard deviations as those on figures 13 and 14, but the highest, or reference, frequency is 100 mc.

Present indications are that the highest frequency usable in an experimental apparatus would be somewhat less than 100 mc—probably around 50 mc—because of practical limitations such as the structural limit on thinness of a crystal, which determines its highest fundamental frequency, and such as the difficulties caused by stray capacitance and inductance at very high frequencies.

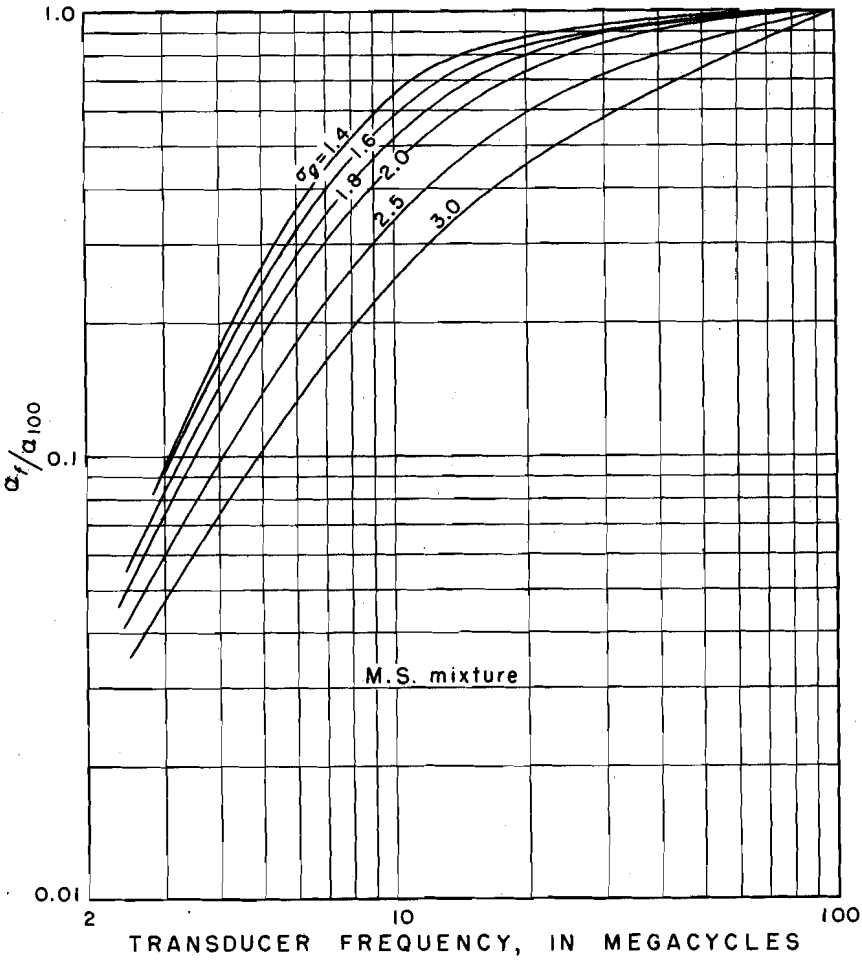

FIGURE 19.—Theoretical curves showing increased sensitivity of measurement of the geometric standard deviation by using a higher reference transducer frequency, for d_g equal to 150 microns.

The sensitivity of the apparatus to concentration measurement depends mainly on the accuracy of readings, the frequency, the geometric mean size, and to a lesser degree on the dispersion parameter. The inherent inaccuracy of reading the apparatus is considerably greater for the larger particle sizes because of the unsteadiness of the echo. If the transducer frequency is 25 mc and the geometric standard deviation is 1.0, the attenuation coefficient at a d_g of 500 microns may be read within 0.15 db per in. to give an accuracy of

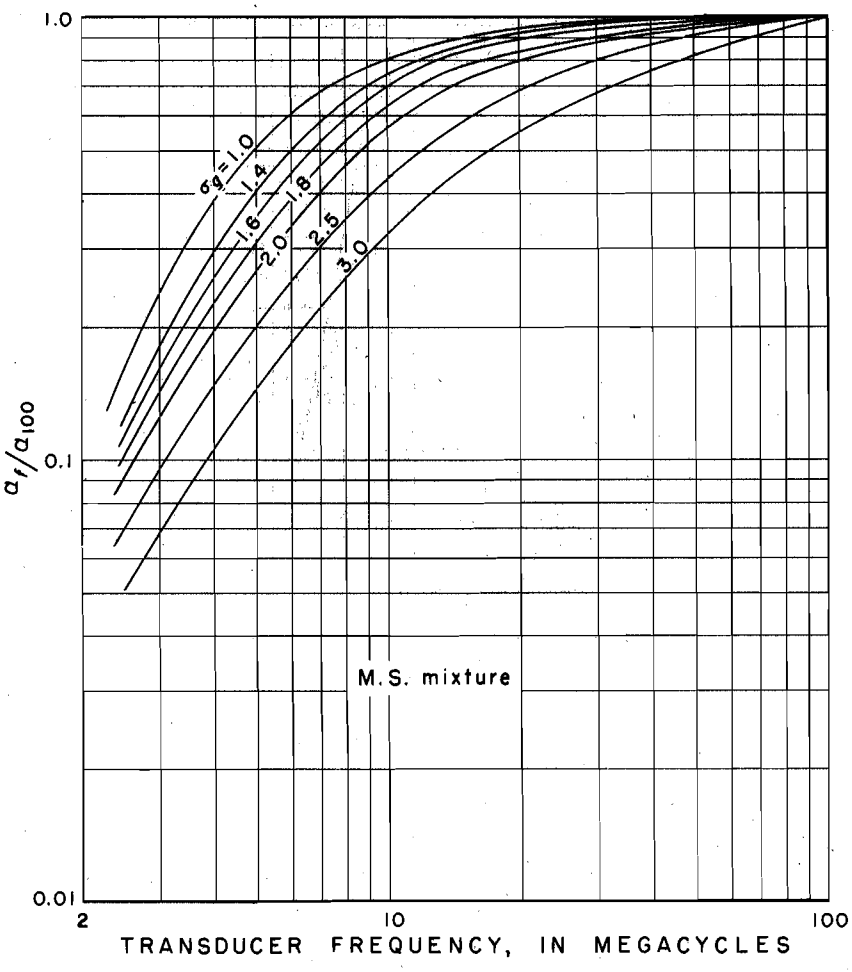

FIGURE 20.—Theoretical curves showing increased sensitivity of measurement of the geometric standard deviation by using a higher reference transducer frequency, for d_g equal to 200 microns.

$\pm$250 ppm, and at a d_g of 100 microns the attenuation coefficient readings are within $\pm$0.05 db per in. for a sensitivity of $\pm$20 ppm. The greatest sensitivity is given by the highest frequency, which therefore should be used for determining concentration. The concentration measurement is then very sensitive for the smaller sizes. The slopes of the attenuation-concentration lines for the six experimental frequencies indicate the sensitivity of the concentration measurement (fig. 21).

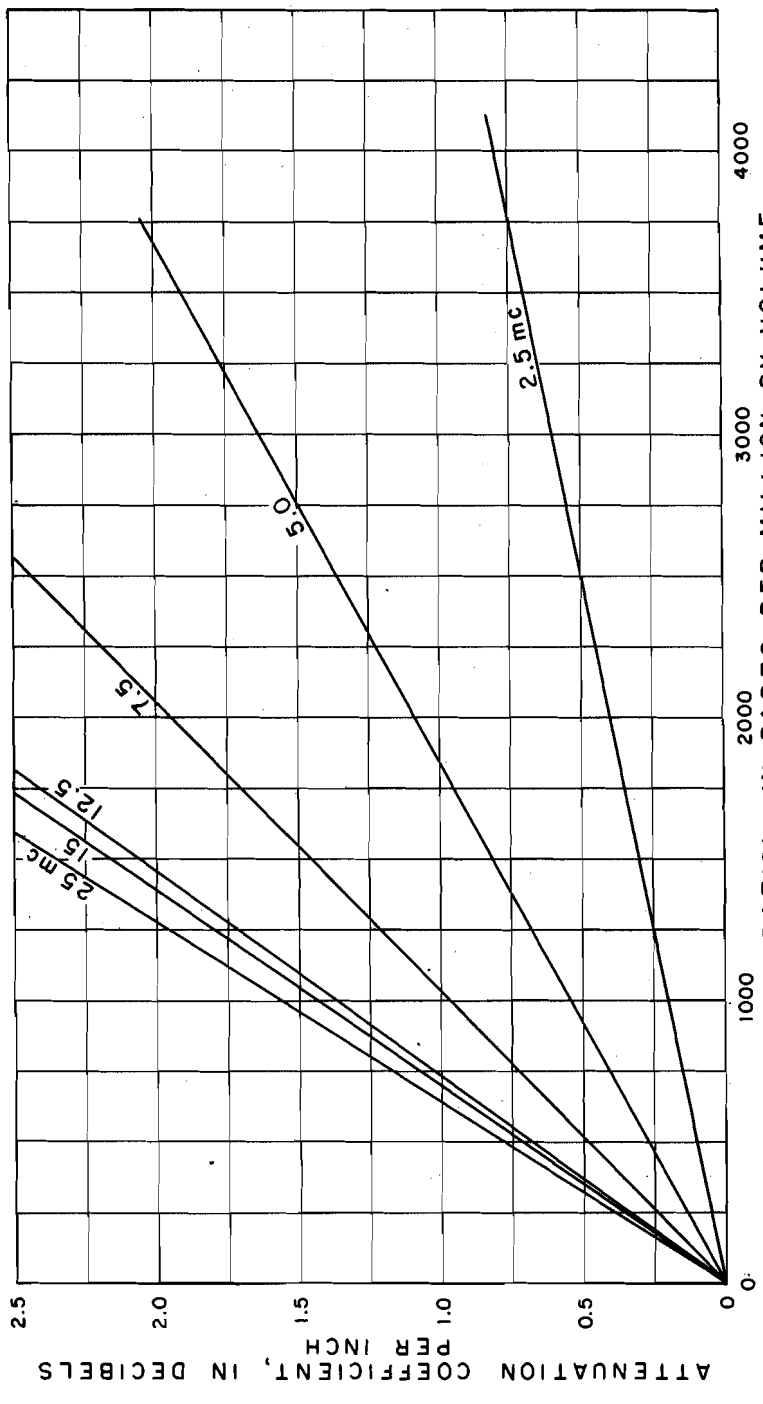

FIGURE 21.—Sensitivity of measurement of concentration for the mixture d_ϵ equal to 200 and σ_ϵ equal to 1.6.

Before the construction of the variable-frequency equipment, some preliminary tests were made of the effects of different types of sediment on the relation of attenuation to particle diameter. These tests were run at 5 and 25 mc, and their results are plotted on figures 22, 23, and 24.

Figure 22 shows the results of tests at 25 mc made on six sands from different sources. The solid line is the theoretical curve for diffraction loss. The respective best-fit diffraction-loss curves would be in rather close agreement except for those of the Cheyenne and Republican River sands.

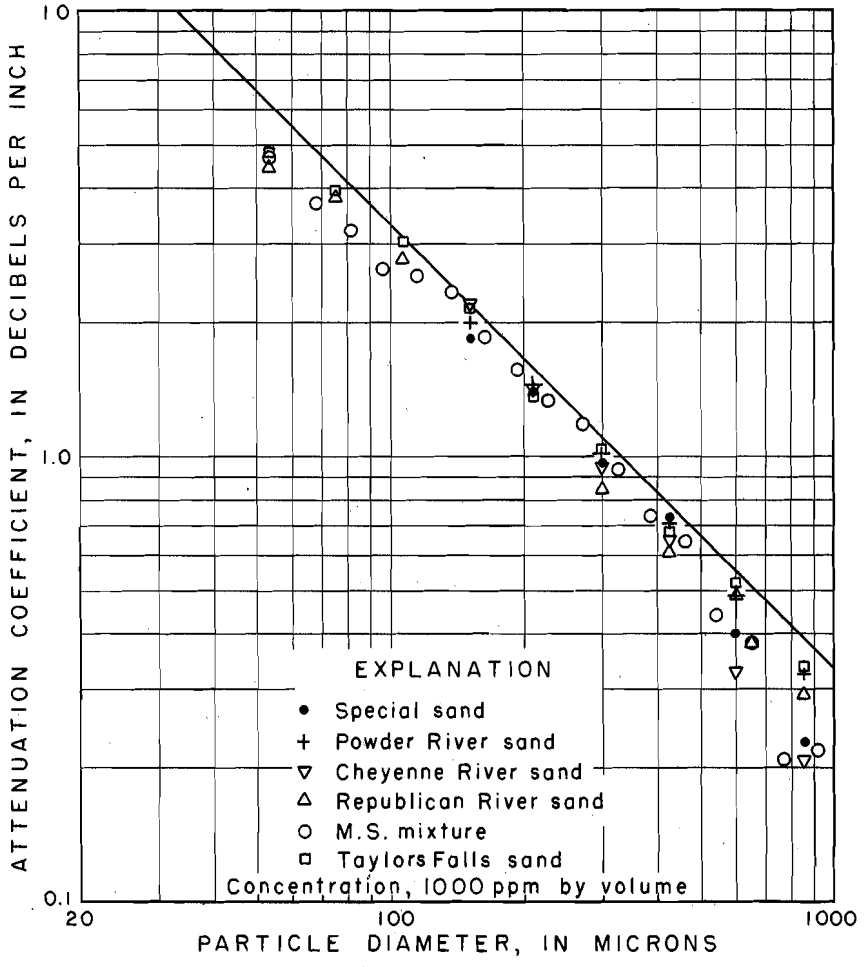

FIGURE 22.—Attenuation-coefficient relation for different sands at 25 mc.

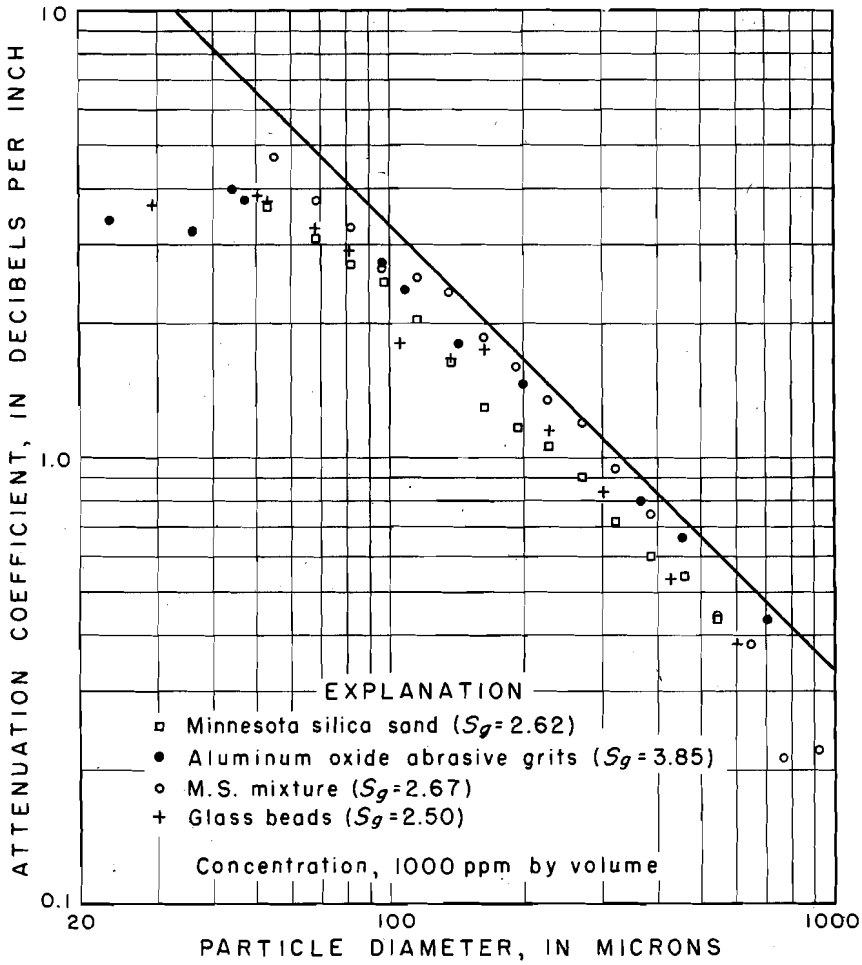

FIGURE 23.—Attenuation-coefficient relation for different sands and materials at 25 mc.

Figure 23 shows the attenuation-diameter relation at 25 mc of M.S. mixture sand, Minnesota silica sand, glass beads, and aluminum oxide abrasive grits. Plotted points for the Minnesota silica sand and glass beads appear to scatter around virtually the same curve. Plotted points for the M.S. mixture and aluminum oxide grit fall about a curve that is of the same slope as the curve for the other two materials but at a different intercept.

The attenuation coefficients for 3 of the 9 sands or other materials began to deviate from their straight-line diffraction-loss curves for sizes larger than 500 microns (figs. 22 and 23). The deviation noted on figure 3 was also for sizes larger than 500 microns. Because the deviation appeared for only three of the sands, some sediment prop-

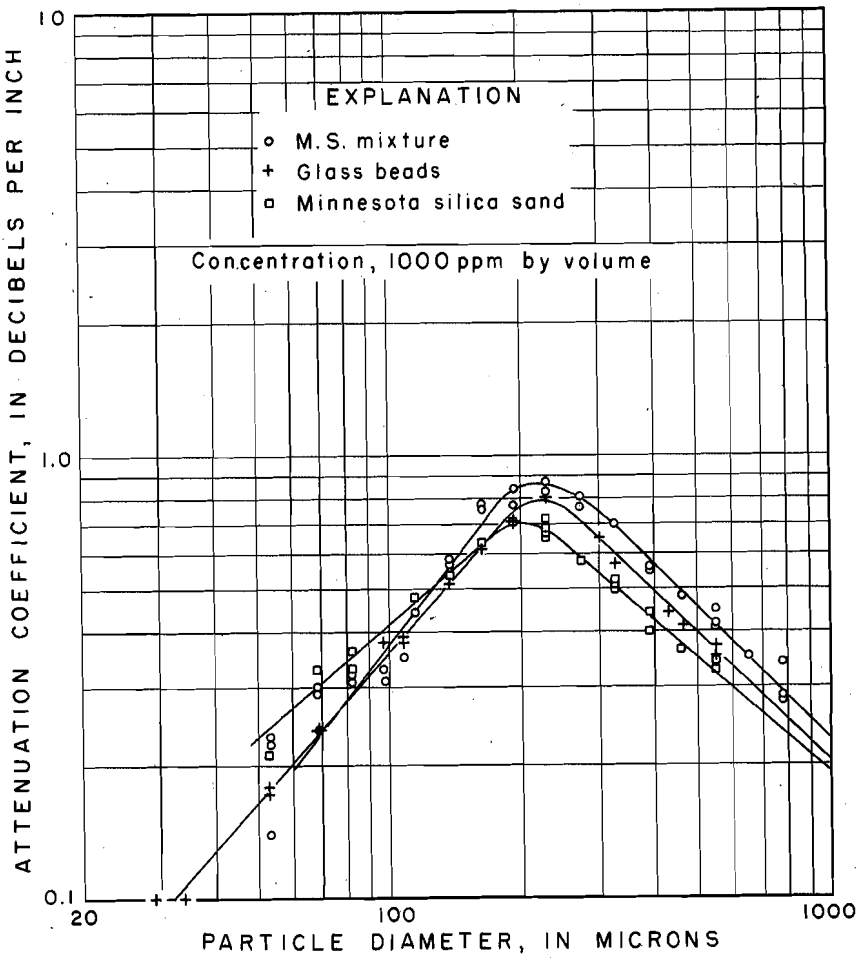

FIGURE 24.—Attenuation-coefficient relation for different materials at 5 mc.

erty must be involved rather than any nonlinearity in the attenuation-concentration relation. The conclusion is that if nonlinearity caused by a high concentration of particles were involved, all the sands and materials would show the same deviation. Further study is needed to determine the reasons for the deviation. However, the deviation is not a serious problem in most laboratory or field testing because only small amounts of the larger sizes are present in most suspended samples and because the attenuation coefficient for the larger sizes is considerably less than that for the sizes smaller than 500 microns. Thus the part of the total attenuation coefficient contributed by the large sizes is usually insignificant.

Figure 23 indicates that attenuation is affected only slightly by density. Shape factors might have some effect, although the turbulence in the chamber would cause all particles to rotate rather than fall with any given orientation. The rotary motion would tend to give a shadow in the diffraction-loss range that would even out some of the angularities except, of course, for elongated particles. Of the materials tested, the abrasive is the most angular, and the glass beads are the most spherical. More work needs to be done to determine the effect of shape factors. Other properties relating to the sonic characteristics (such as the modulus of elasticity) of a material also should be considered. An important aspect of future research on this subject is the determination of the influence of different sediment characteristics on the measured results.

Figure 24 shows the attenuation-diameter relation for the M.S. mixture, Minnesota silica sand, and glass beads at 5 mc. The slope of Minnesota silica sand in the diffraction-loss range is different from the theoretical slope. The slopes for all three materials differ in the transition range.

Although the ultrasonic method is promising for rapid and convenient analysis of sediment concentration and particle size, the present form of the equipment is not very practical, especially when finer sediments are involved. Too much time is required for the sediment to settle out before the echo of the next frequency can be adjusted to the zero-concentration level. The settlement time is so great that drift can be a serious problem. In fact, reproducible data were difficult to obtain for sizes smaller than about 60 microns. Unfortunately, equipment limitations and the unavailability of sediments with very small, but known, particle sizes prevented extension of the study into the viscous-loss range.

To design a transmitter that would be free of these problems seems entirely possible. Instead of several plug-in units the transmitter should be a single unit that has crystal-controlled channels that are band-switched to obtain the required frequencies. Because all tubes would be in constant operation, the single unit would eliminate the warmup time before each test and the associated drift. Also, the transmitter would be designed for higher power output than that of the present units; thus higher frequencies could be used to improve the sensitivity of measurement. A stable transmitter could be adjusted at each frequency to give a certain exact output for zero concentration; thus, the zero-level adjustments would be eliminated except for periodic checks. Rapid tests on any size of sediment would then be possible.

An adequate ultrasonic method would be especially advantageous for sediments finer than the sieve range, because the ultrasonic

analysis could be completed in a few minutes, whereas a sedimentation-method analysis takes considerable time. The distribution for the complete range of particle sizes could be determined with the method if the experimental attenuation-diameter relations are extended into the viscous-loss range and if the procedures outlined in this study are followed. Also, distributions other than log normal could be determined with the method if they were used to plot curves corresponding to those on figures 7 to 14.

The ultrasonic method seems to be adaptable to a continuously recording device for use in natural streams. The housing containing the transducer could be suspended in the stream at the desired point of measurement. The equipment could operate principally at one frequency, for instance 50 mc, and could be made to scan the range of frequencies automatically at preset time intervals. Hence, a continuous record of concentration with frequent size analyses could be read from the recorder graphs.

Some method would have to be found for correcting the zero-concentration calibration of a field instrument for the effects of temperature and entrained air. A possible solution would be to trap a sample of water, let the sediment settle out, and then make the zero reading.

Because the attenuation relations for light and sound differ only by a constant factor, the approach described in this study seems to be equally adaptable to light. However, the experimental curves for light would probably differ more from one sediment to another than the curves for sound (fig. 3). Thus, quantitative measurement of size distribution and concentration probably could be obtained for a given sediment by varying the wavelength of the light, as did Gamble and Barnett (1937).

CONCLUSIONS AND RECOMMENDATIONS

A method was theoretically developed and experimentally verified for measuring concentration and size distribution of a suspended sediment with ultrasonic equipment.

In the theoretical development, attenuation relations for sound waves passing through suspensions of uniform-sized particles were extended to include size-distribution parameters describing mixtures of particle sizes having a log-normal distribution. From the relations for mixtures of particle sizes, the size-distribution parameters and the concentration were determined uniquely by varying the frequency of the sound wave. The derived relations seem equally adaptable to methods in which light waves are used. Furthermore, size distributions other than log normal can be determined by following a method similar to that described here.

For the diffraction-loss range, the theoretical attenuation is independent of frequency, but the experimental results show that attenuation is a function of the one-third power of frequency. No simple theoretical relations are available for the attenuation coefficient in the transition region between the scattering-loss and diffraction-loss ranges. The experimental relations showed about the same dependency on frequency as did those for light waves. The attenuation equation for the M.S. mixture sand in the transition region was

$$\alpha = 0.36K^{2.4}d^{1.3}C$$

For light, the attenuation coefficient is proportional to K^2, whereas for sound it is proportional to $K^{2.4}$. Experimental relations for the scattering-loss and viscous-loss ranges were not found because of equipment limitations. Sizes tested covered the sieve range only.

Experimental results from artificially constructed log-normal distributions were in close agreement with the theoretical results.

The sensitivity of measuring the geometric mean size is high, but that of measuring the geometric standard deviations should be increased by using a frequency higher than 25 mc. The ultrasonic technique is sensitive to concentration for the usual range of suspended-sediment sizes.

The time required for an ultrasonic analysis in the laboratory will be considerably shorter than that required for a sedimentation-method analysis, especially of sizes smaller than the minimum sieve size. However, the drift that occurs in the present equipment must be reduced before the equipment will be practical for fine sediments. Equipment limitations and the unavailability of fine sediments with known particle sizes prevented adequate study of the viscous-loss range.

The ultrasonic method seems adaptable to continuously recording and automatic field installations. Operation at one frequency, perhaps 50 mc, could be augmented by scanning the range of frequencies at preset time intervals to give a record of concentration with frequent size analyses.

Although experimentally verified, the ultrasonic method still requires extensive research before it will be usable for routine work in the laboratory or field. An extensive equipment-development program is needed to improve the laboratory equipment and to design continuously recording field equipment. With improved laboratory equipment, the experimental relations and theoretical curves can be extended into the viscous-loss range. The effects on the attenuation-coefficient equation of such factors as shape, density, and thermal and

elastic properties of the particle should be studied for each loss range. Allowable limits of departure of size distribution from a log-normal curve need to be studied.

LITERATURE CITED

Anderson, V. C., 1950, Sound scattering by solid cylinders and spheres: Acoustical Soc. America Jour., v. 22, no. 4, p. 426–431.

Austin, J. B., 1939, Methods of representing distribution of particle size: Indus. and Eng. Chemistry, Anal. Ed., v. 11, p. 334–339.

Blench, Thomas, 1952, Normal size distribution found in samples of river bed sand: Civil Eng., v. 22, no. 2, p. 147.

Busby, J., and Richardson, E. G., 1955, The propagation of ultrasonics in suspensions of particles in a liquid: Phys. Soc. [London] Proc., v. 69, no. B, p. 193–202.

Chow, Ven Te, 1954, The log-probability law and its engineering applications: Am. Soc. Civil Engineers Proc., Separate no. 536, 25 p.

Colby, B. R., and Hembree, C. H., 1955, Computations of total sediment discharge, Niobrara River near Cody, Nebraska: U.S. Geol. Survey Water-Supply Paper 1357, 187 p.

DallaValle, J. M., 1948, Micrometrics: New York, Pitman Pub. Co., 555 p.

Einstein, H. A., 1944, Bed load movement in Mountain Creek: U.S. Dept. Agr., Soil Conserv. Service, SCS–TP–55, 54 p.

Epstein, P. S., 1941, On the absorption of sound waves in suspensions and emulsions (Theodore von Karman Anniv. volume): California Inst. Technology, Pasadena, Calif., p. 162–188.

Faran, J. J., 1951, Sound scattering by solid cylinders and spheres: Acoustical Soc. America Jour., v. 23, no. 4, p. 405–417.

Gamble, D. L., and Barnett, C. E., 1937, Scattering in the near infrared—a measure of particle size and size distribution: Indus. and Eng. Chemistry, Anal. Ed., v. 9, p. 310–314.

Grassy, R. G., 1941, Use of turbidity determinations in estimating the suepended load of natural streams: Am. Water Works Assoc. Jour., v. 35, no. 4, p. 439–453.

Hatch, Theodore, and Choate, S. P., 1929, Statistical description of size properties of non-uniform particulate substances: Franklin Inst. Jour., v. 207, p. 369–387.

Lord Rayleigh, 1937, The theory of sound, 2d ed.: New York, Dover Pub., v. 2, 504 p.

Morse, P. M., 1948, Vibration and sound, 2d ed.: New York, McGraw-Hill Book Co., 468 p.

Morse, P. M., and others, 1946, Scattering and radiation from circular cylinders and spheres: U.S. Navy Dept., Office of Research and Inventions, Washington, D.C., 129 p.

Sewell, C. J. T., 1910, The extinction of sound in a viscous atmosphere by small obstacles of cylindrical or spherical form: Royal Soc. [London] Philos. Trans. (A), v. 210, p. 239–270.

Smoltczyk, H. U., 1955, Beitrag zur ermittlung der feingeschiebe mengenganglinie: Inst. fur Wasserbau Mitt. 43, Technischen Univ. Berlin-Charlottenburg [in German], p. 25–60.

Stakutis, V. J., and others, 1955, Attenuation of ultrasound in aqueous solutions: Acoustical Soc. America Jour., v. 27, no. 3, p. 539–546.

Stutz, G. F. A., 1930, The scattering of light by dielectrics of small particle size: Franklin Inst. Jour., v. 210, p. 67–85.

Traxler, R. N., and Baum, L. A. H., 1935, Measurement of particle size distribution by optical methods: Am. Standard Testing Materials Proc., v. 35–II, p. 457–467.

Uriek, R. J., 1948, The absorption of sound in suspension of irregular particles: Acoustical Soc. America Jour., v. 20, no. 3, p. 283–289.